NOV 1968
RECEIVED
NASA STI FACILITY
INPUT BRANCH

HQ NASA LIBRARY
WASHINGTON 25, D. C.
STOP 85

JET PROPULSION LABORATORY
CALIFORNIA INSTITUTE OF TECHNOLOGY
PASADENA, CALIFORNIA

FACILITY FORM 602

N68-88643
(ACCESSION NUMBER)

(THRU)

85
(PAGES)

None
(CODE)

CR 97411
(NASA CR OR TMX OR AD NUMBER)

(CATEGORY)

RE-ORDER NO. 63-39

NATIONAL AERONAUTICS AND SPACE ADMINISTRATION
CONTRACT NO. NAS 7-100

Internal Office Memorandum
Translation No. 33

THE PHYSICS OF NUCLEAR FISSION

(Sections 5 - 8)

A. Kraut

Translated by Dorris Wallenbrock from
Nucleonik, Vol. 2, June 1960

Copy No._____

JET PROPULSION LABORATORY
CALIFORNIA INSTITUTE OF TECHNOLOGY
PASADENA, CALIFORNIA
February 15, 1963

CONTENTS

5. Kinetic Energy of the Fission Products 1

5.1 The Kinetic Energy of Fission Products Within the Framework of Energy Balance 1

5.2 Measured Energy Magnitudes and Their Correlation 3

5.3 Kinetic-Energy Distribution of Individual Fission Products 6

5.4 Range Distribution of Individual Fission Products in Absorbers 8

5.5 Distribution of the Total Kinetic Energy $T_l + T_h$ for the Fixed Fission Ratio A_h/A_l 9

5.6 The Total Kinetic Energy of All Fission-Product Pairs 13

6. Anisotropy of the Fission-Fragment Emission 15

6.1 Introduction 15

6.2 Photofission 16

6.3 Thermal Fission of Oriented Nuclei 18

6.4 Fission by Neutrons With Energies 0.4 MeV $\lesssim E_n \lesssim$ 10 MeV 19

6.5 Fission by Particles With Energies $E < 10$ MeV 21

7. Nuclear Charge of the Fission Products 27

7.1 Introduction 27

7.2 Measured Results 28

7.3 Postulate for the Charge Distribution for Fixed Mass Number 29

7.4 Proof of the Postulates 31

CONTENTS (Cont'd)

8. Prompt Neutrons and Gamma Rays 35

8.1 Introduction 35

8.2 Prompt Neutrons 36

8.3 Prompt Gamma-Radiation 48

References 52

TABLES

5.2 Measurements of the energy distribution and range of fission products 61

6.1 Measurements of the anisotropy of fission-fragment emissions 62

7.21-1 Specific independent and specific cumulative yields of fission products for spontaneous and thermal fission . . . 63

7.21-2 Measurement of independent yields of fission products at bombardment energies E > 5 MeV 64

8.211 Mean number of neutrons emitted per fission for spontaneous and thermal fission 65

8.212 Mean numbers of neutrons emitted per fission for fission by neutrons 66

8.22 Measurements and computations of the energy spectra of prompt neutrons 67

8.23 Measured probable emission of exactly ν neutrons per fission 68

8.3 Measurements and computations for prompt gamma-radiation 69

FIGURES

5.21-1 Contour diagram for the thermal or spontaneous fission of the compound nucleus Pu^{242} (Sm 57-1) 70

FIGURES (Cont'd)

5.22-2 Distribution of the total kinetic energy of the fission products for various areas of the fission ratio in the thermal or spontaneous fission of the compound nucleus Pu^{242} (Sm 57-1) 70

5.3 Distribution of the kinetic energy of individual fission products in the fission of U^{235} by neutrons of various energies 70

5.53-1 Most probable total kinetic energy of the fission product as a function of the fission ratio for the fission of Bi and Ta by 450-MeV protons 71

5.53-2 Mean energy magnitudes (averaged like $\overline{T_l + T_h}$) as functions of the fission ratio for the spontaneous fission of Cf^{252} (St 58-3) 71

5.6 Mean total kinetic energy of all fission-fragment pairs as a function of $Z_z^2/A_z^{1/3}$, computed from a number of data (Table 5.2; Te 59-1) 72

6.21 Anisotropies in the photofission of various nuclei as a function of the maximum energy of the continuous radiation (Wi 56-1) 72

6.4 Anisotropy of the fission-fragment emission and effective cross section for the fission of Th^{232} by neutrons as a function of their energy (He 56-1) 72

6.52 Anisotropy of the fission-fragment emission for the fission of various target nuclei by deuterons and α-particles as a function of parameter Z^2/A of the compound nucleus (Co 58-2) 73

6.53 Anisotropy of the fission-fragment emission in fission by very fast protons as a function of their energy (Ha 59-1) 73

6.54 Anisotropy in fission by 22-MeV protons as a function of the fission ratio (Co 55-1) 74

7.41-1 Charge distribution for fixed mass number in the thermal fission of V^{235} according to postulate b 75

FIGURES (Cont d)

7.41-2 Charge distribution for fixed mass number in thermal fission according to postulate b 76

7.41-3 The most probable charge $<Z>$ for isobars of a mass number A as a function of A, according to Wa 58-1 76

7.42 Charge distribution for fixed mass number as a function of bombardment energy (Pa 58-1) 77

8.212 $\bar{\nu}$ for several target nuclei and the spontaneously splitting nucleus Pu^{240} as a function of the bombarding-neutron energy (Le 58-1+) 77

8.213-1 Relative probability of neutron emission from light and heavy fission fragments and from both types of fission fragments as a function of the fission ratio for the thermal fission of U^{233} (Fr 54-1) 78

8.213-2 Number of neutrons emitted from one fission fragment as a function of the mass number of this fission fragment in the spontaneous fission of Cf^{252} (Wh 59-1) 78

8.214 $\bar{\nu}$ as a function of the total kinetic energy of the fission products in the spontaneous fission of Cf^{252} 79

8.22 Measured energy spectrum and computed energy spectra of prompt neutrons in the spontaneous fission of Cf^{252} (Te 59-1) 79

8.23 Measured and computed probability for the emission of exactly ν neutrons as a function of ν for the spontaneous fission of several nuclei (Le 56-2) 80

8.32 Energy spectrum of the prompt gamma-radiation in the thermal fission of U^{235} and the spontaneous fission of Cf^{252} 80

THE PHYSICS OF NUCLEAR FISSION

by A. Kraut

Translated by Dorris Wallenbrock

5. KINETIC ENERGY OF THE FISSION PRODUCTS

5.1. The Kinetic Energy of Fission Products Within the Framework of Energy Balance

The kinetic energy $T_L + T_H$ of the two fission fragments appears to stem essentially from the Coulomb energy between the fission fragments (considered in terms of the point at which the latter already exist but have not yet separated). $T_L + T_H$ is nearly independent of the bombardment energy and, thus, of the excitation of the splitting nucleus (¶ 5.6), and a rough estimate of the Coulomb energy is known to yield a value which agrees with the measured mean values of $T_L + T_H$ (¶ 5.6). The deformation energy of the fission fragments (at that point at which they already exist but have not yet separated) would then have to be transformed into excitation energy. Following this transformation, let U_L and U_H be the excitations of the light and heavy fission fragments, respectively.

$U_L + U_H$ supplies the energy for the emission of prompt neutrons and gamma-rays (¶ 8):

$$U_L + U_H = \Sigma B_n + \Sigma T_n + \Sigma T_\gamma$$

It is assumed here that the fission products (i.e., the fission fragments after the emission of the prompt neutrons) exist in the ground state, after the entire prompt gamma-radiation has been emitted. Deviations from this assumption would not result in any great errors, because the excitations of isomeric nuclei are generally small compared with $U_L + U_H$.

The energy liberated during fission is

$$F = T_L + T_H + U_L + U_H \tag{5.1-2}$$

F does not contain the energy of the light particles which may have been emitted before fission (¶ 1.33 and 1.43), nor the energy liberated through the β-emission or K-capture or the emission of delayed neutrons on the part of the fission products; however, it does contain the binding energy of the prompt neutrons.

Within the limits of measurement accuracy, the kinetic energy of fission fragments and fission products* can often be equated; then,

$$F = T_l + T_h + U_L + U_H \tag{5.1-3}$$

On the other hand, if Equation (5.1-3) is valid,

$$F = \begin{cases} c^2 (M_z - M_L - M_H) \\ \text{for spontaneous fission,} \\ c^2 (M_z - M_L - M_H) + E_n + B_n \\ \text{for fission by slow neutrons.} \end{cases} \tag{5.1-4}$$

*Capital subscripts refer to fission fragments; lower-case subscripts refer to fission products.

M_z, M_L, and M_H denote the ground-state masses of the compound nucleus, the light fission fragment, and the heavy fission fragment; E_n and B_n are the kinetic and binding energies of the bombarding neutron.

In establishing the conservation theorem for mass numbers A and momentum Av, the following approximations are usually applicable:

$$A_l + A_h + \bar{\nu} \cong A_z, \tag{5.1-5}$$

$$A_l v_l = A_h v_h \tag{5.1-6}$$

(Eq. 5.1-6 is written for fission products instead of fission fragments.) The equations carry the further restriction that the projectile energy be so small that the projectile momentum can be neglected and a compound nucleus is formed. Also,

$$A_l T_l = A_h T_h \tag{5.1-7}$$

On the basis of the above equations, one can calculate, for a pair of complementary (originated in the same act of fission) fission products, the masses and energies from the velocities and the velocities and masses from the energies.

5.2. Measured Energy Magnitudes and Their Correlation

5.21. Measurements of fission-product pairs.

Measurements of T_l and T_h in the case of fission-product pairs (i.e., fission products originating from a

single act of fission) are shown in contour diagrams (Fig. 5.21-1). The contour lines are curves of equal frequency of pairs of fission products with energies between T_l and $T_l + dT_l$ or between T_h and $T_h + dT_h$. The group of diagonally rising lines consists of lines of constant T_l/T_h; if the bombardment energy is sufficiently low, they are also constants of the fission ratio A_h/A_l (Eq. 5.1-7) and the mass numbers A_l and A_h (Eq. 5.1-5). The group of diagonally descending lines consists of lines of constant $(T_l + T_h)$.

If we cut the contour diagram (visualized as three-dimensional), with a plane vertical to the drawing plane, along a line T_l/T_h = const, the distribution of $T_l + T_h$ <u>for a fixed fission ratio</u> A_h/A_l results (if the bombardment energy is sufficiently small). Figure 5.21-2 shows such distributions for the fission of the compound nucleus Pu^{242}. The value of $T_l + T_h$ at the maximum is the most probable total kinetic energy $\langle T_l + T_h \rangle$ for the A_h/A_l under consideration. In addition, the mean total energy $T_l + T_h$ can be calculated for each A_h/A_l. By averaging $T_l + T_h$ over all A_h/A_l, weighted by the frequency of the appropriate A_h/A_l (of the area below the distribution curve), the mean total kinetic energy $\overline{\overline{T_l + T_h}}$ of all fission-product pairs is yielded.

If we drop the difference between T_l and T_h, i.e., consider only the frequency of measured fission-product energies between T and T + dT as a function of T, then we obtain the distribution of the energy T of individual fission products. Such distributions are shown in Fig. 5.3.

Using ¶ 5.1, the mass numbers A_l and A_h and the velocities v_l and v_h, and concurrently, the distributions of A (primary mass distribution; see ¶ 4.1) and of v (velocity distribution), can be determined from T_l and T_h.

Measurements of v_l and v_h of fission-product pairs are shown in similar contour diagrams, whose coordinates are v_l and v_h. Using ¶ 5.1, they can be converted into T_l-T_h-contour diagrams, and thus, all the magnitudes in ¶ 5.21 are again obtained.

Table 5.2 gives a general view of the energy and velocity measurements carried out on fission-product pairs.

5.22. Measurements of fission products without consideration of their paired origin.

Measurements of the kinetic energy T of individual fission products yield only the distribution of T; such measurements are shown in Table 5.2. Measurements of the velocity v of individual fission products yield only the distribution of v. The latter was determined in this manner

only for the thermal fission of U^{233}, U^{235}, and Pu^{239} (Le 52-1).

5.23. Measurements of fission products with fixed mass number.

Measurements of energy T_l of fission products with a fixed mass number A_l can, according to ¶ 5.1, also yield A_h and T_h, assuming a sufficiently low bombardment energy, and thus, the distribution of $T_l + T_h$ for one fixed fission ratio A_h/A_l. Correspondingly, this is true when subscripts l and h are interchanged. The measurements performed pertain to the fission of Bi by protons with energies between 50 and 2,200 MeV (Su 56-1) and the fission of Bi and Ta by 450-MeV protons (Po 57-2); for such bombarding energies, the equations of ¶ 5.1 are no longer valid. Thus, in Po 57-2, A_h was estimated with the aid of the measured distribution of the fission-product masses (Table 4.21), after A_l had been measured. Finally, on the basis of the energy and impulse balance, the most probable kinetic energy $\langle T_l + T_h \rangle$ was determined (Fig. 5.53-1).

5.3. Kinetic-Energy Distribution of Individual Fission Products

Figure 5.3 shows the shape of the energy distribution during the fission of U^{235} by neutrons of various energies E_n. The transition from a double-hump curve to a single-hump curve with increasing E_n corresponds

to the parallel change in the mass distribution (¶ 4.221). The same transition takes place with the target nucleus Ra^{226} in the far narrower E_n region of 3 to 15 MeV (No 58-1).

The two energy-distribution maxima move closer together with increasing bombardment energy, and thus also with increasing excitation of the splitting nucleus (Fig. 5.3). This is clearly demonstrated in the comparison between the energy distribution for the spontaneous fission (Ko 58-4) and the photofission (Ko 56-1, Ko 59-1) of U^{238}: The distance between the maxima is smaller in photofission.

For compound-nucleus excitations $U_z \lesssim 5$ MeV, the energy distribution depends only slightly upon U_z. Thus, the energy distributions for thermally split U^{239} and spontaneously splitting Pu^{240} (Se 54-1, Mo 58-1), as well as those for thermally split Pu^{241} and spontaneously splitting Pu^{242} (Sm 57-1) are not markedly different.

With constant U_z, the energy distribution does not manifest a strong dependence on mass number and atomic number Z_t of the target nucleus (for $Z_t > 90$) any more than does the mass distribution. This is clearly visible in the contour diagram for the spontaneous fission of Pu^{242}, Cm^{242}, and Cf^{252}.

From the above, it is apparent that a single-hump (double-hump) energy-distribution curve corresponds to a single-hump (double-hump) mass-distribution curve. There are still other mathematical interrelationships which are valid for <u>both</u> types of distributions. However, one must not conclude from this that the double-hump energy distribution is an

inversion of the double-hump mass distribution: A very heavy fission product is generated, together with a very light fission product; a heavy fission product with above-average energy T_s, on the other hand (see Fig. 5.21-1), is preferably paired with a light fission product with above-average energy T_l.

5.4. Range Distribution of Individual Fission Products in Absorbers

In the case of very high bombardment energies, it is difficult to measure energy distributions of fission products. Therefore, range distributions were frequently measured in photoemulsions and interpreted under the assumption that the number of maxima corresponds for range, energy, and mass distribution and that a narrow (broad) range distribution corresponds to a narrow (broad) energy and mass distribution. Those measurements of range distribution which have been interpreted in this manner as substitutes for energy distributions are shown in Table 5.2. At similarly high bombardment energies (¶ 4.221 and 4.24), they then lead to similar results as measurements of the mass distribution.

In the case of the target nuclei U^{238} and Bi^{209}, the probability of equal ranges of the two fission products increases with the increasing excitation U_k of the residual nucleus remaining after the cascade, until U_k has reached 60 to 100-MeV; with higher U_k, the range distribution becomes broader again (Pe 55-1, Ša 55-2). In the fission of Bi by 660-MeV protons, a U_k region is reported in which the range distribution appears to be

three-humped (Da 59-1). The range distributions for the fission of uranium by 350-MeV protons (Iv 56-2, Iv 57-1), 280-MeV-π^+ mesons, and slow π^- mesons (Be 55-1, Pe 55-1, Pe 55-4, Iv 56-3, Iv 57-1) are single-humped and nearly equal (Iv 58-1, Iv 58-2).

With very light target nuclei (Ag, Br) and high bombardment energies (E_p = 300 - 660 MeV), the range distribution also has an appearance similar to that of the mass distribution (¶ 4.24): One maximum corresponds to the fissions, and two outer maxima (Šа 58-1) correspond to the spallations.

A systematic discussion of the ranges of fission products in absorbers is not the object of this paper.

5.5 Distribution of the Total Kinetic Energy $T_l + T_h$ for the Fixed Fission Ratio A_h/A_l.

5.5.1 Width of the distribution.

The width of the distribution can be determined for each ratio A_h/A_l from the measurements of T_l and T_h or v_l and v_h of fission-product pairs (Table 5.2, ¶ 5.21). For individual fission ratios, the width of the distribution was also determined in an indirect manner for the thermal splitting of U^{235} (Co 56-1) and for the fission of U^{233} and U^{235} by fission neutrons (Go 56-1). Figure 5.21 shows the distribution as a function of A_h/A_l for the fission of the compound nucleus Pu^{242}.

In all cases, the width of the distribution turns out to be about 10 to 13% of the probable total energy $\langle T_l + T_h \rangle$. The width of the distribution does not necessarily appear to depend on the splitting nucleus and the fission ratio; only in the case of Cf^{252} was a weak minimum observed at the most probable A_h/A_l (Mi 58-1). The statistical theory (Fo 56-1) gives the inadequate value of 6% of $\langle T_l + T_h \rangle$ for the width of the distribution.

5.52 Interpretation of the distribution.

The simplest explanation for the fact that the total kinetic energy can assume a whole range of values with a fixed fission ratio would be based on the fact that the nuclear charges of the fission product can have several values, which result in various Coulomb energies, and thus (¶ 5.1), in different $T_l + T_h$. If we assume the excitation $U_L + U_H$ of the fission fragments to be constant, the distribution of $T_l + T_h$ and the distribution of the nuclear charge (both with fixed A_h/A_l, and hence, fixed mass numbers A_l and A_h; see ¶ 7.1) obviously determine each other (Eqs. 5.1-3 and 5.1-4). However, calculations showed that the charge distribution resulting from the $(T_l + T_h)$ distribution is completely incompatible with the measured charge distribution (¶ 7.41; Br 49-1; with new energy values: Mi 56-1),

and that a much too small ($T_l + T_h$) distribution (Mi 56-1) follows from the measured charge distribution. Thus, the fluctuations in $T_l + T_h$ must stem primarily from the fluctuation of the excitation $U_L + U_H$, even though the total amount of $T_l + T_h$ is given primarily by the Coulomb energy (¶ 5.1).

Fluctuations of $U_L + U_H$ correspond to fluctuations of the energy yielded in the form of prompt neutrons and gamma-rays (Eq. 5.1-1). From the distribution of $U_L + U_H$, the evaporation theory yields the probability for the emission of exactly ν neutrons per fission as a function of ν (¶ 8.23). If the calculation is based on that distribution of $U_L + U_H$ which, according to Eq. (5.1-3), results from the measured ($T_l + T_h$) distribution, the probability for the emission of the exactly ν neutrons per fission agrees satisfactorily with the measured probability (Le 56-2, ¶ 8.23).

If, on the other hand, we consider the measured probability for the emission of exactly ν neutrons per fission on the basis of being a function of ν, then calculate the distribution of $U_L + U_H$, and finally, from this, according to Eq. (5. 1-3), the distribution of $T_l + T_h$, 11% of the most probable total energy (Co 56-1) is yielded as the width of this last distribution. The value measured in Co 56-1 amounts to 11.4%.

5.53. <u>The most probable and mean total kinetic energy</u>.

The most probable total kinetic energy $\langle T_l + T_h \rangle$ and the mean total kinetic energy $\overline{T_l + T_h}$ (¶ 5.21) differ only slightly and will not always be kept strictly apart. They should increase with a decreasing A_h/A_l if $T_l + T_h$ stem from the Coulomb energy of the fission fragments (¶ 5.1): The Coulomb energy is proportional to the product $Z_L Z_H$ of the fission-fragment charges, and, because of the condition $Z_L + Z_H$ = const, this product has a maximum for $Z_L = Z_H$, i.e., for a symmetrical splitting.

Actually, the maximum of $\langle T_l + T_h \rangle$ exists only with high bombardment energies $E \gtrsim 20$ MeV for $A_h/A_l = 1$. Figure 5.3-1 shows this for the fission of Ta and Bi by 450-MeV protons (Po 57-2). The range of the fission products reaches a maximum of $\overline{T_l + T_h}$ at $A_h/A_l = 1$ as a function of A_h/A_l (Do 54-1) in the fission of U^{238} by 18-MeV deuterons and 335-MeV protons.

In thermal and spontaneous fission, the maximum of $T_l + T_h$ is at $A_h/A_l \simeq 1.2$. Figure 5.53-2 shows this for Cf^{252} (St 58-3; also, Hi 57-1 and Mi 58-1). Similar results were found for the thermal fission of Th^{229} (Sm 58-1), U^{233} (Br 50-1, Fr 54-1, St 57-1) U^{235} (Br 50-1, St 57-1), and Pu^{239} (Br 50-2, St 57-1). A similar maximum can be

assumed from the shape of the fission-product range dependent upon A_h/A_l (thermal fission of Pu^{239}, Ka 48-1).

Thus far, theory has been unable to explain this position of the maximum. In Fig. 5.53-2, the sum $\overline{F}$, computed from the mean kinetic and mean excitation energies (the latter average was $\overline{T_l + T_h}$), once using Eq. (5.1-3) and once Eq. (5.1-4), is entered as a function of A_h/A_l.

The two curves agree satisfactorily for $A_h/A_l > 1.1$, but not at all for $A_h/A_l < 1.1$. The only suggested explanations offered so far are the dependence of the measured results on A_h/A_l (Mi 56-1) and large systematic errors in measuring the fission products, which are rarely even close to symmetrical (St 58-3).

In Fig. 5.53-2, $\overline{U_L + U_H}$ shows no maximum for the most probable fission ratio $A_h/A_l \simeq 1.35$. This is contradictory to the statistical theory of fission (Fo 56-1).

5.6. The Total Kinetic Energy of All Fission-Product Pairs

The mean total kinetic energy $\overline{\overline{T_l + T_h}}$ of all fission-product pairs is derived, according to ¶ 5.21, from the contour diagrams or through direct calorimetric measurement (Le 55-1, Gu 57-1). If we take into account mathematically the emission of prompt neutrons, we can also determine the mean kinetic energy $\overline{\overline{T_L + T_H}}$ of all fission fragments (before

neutron emission). Sometimes, a most probable total kinetic energy, which is not further defined, is given. The differences between the individual values are small and often insignificant.

Computed optimum values for $\overline{\overline{T_L + T_H}}$ (Te 59-1) can be read from Fig. 5.6 by averaging numerous measurement data.

From an over-all point of view, $\overline{\overline{T_l + T_h}}$ increases with increasing nuclear charge Z_t of the target nucleus (Sm 58-2 for $Z_t \geqq 90$, Ju 49-1 and Po 57-2 for $Z_t \leqq 90$). The Coulomb energy between the fission fragments, of course, increases in the same direction.

With moderate excitation of the compound nucleus $U_z \lesssim 8$ MeV and $90 \leqq Z_z \leqq 98$, $\overline{\overline{T_L + T_H}}$ depends roughly linearly on the theoretically meaningless parameter $Z_z^2/A_z^{1/3}$ (Fig. 5.6 for Te 59-1; Sm 57-1). As a function of Z_z^2/A_z, $\overline{\overline{T_l + T_h}}$ yields a rising curve for $90 \leqq Z_z \leqq 98$ but is followed by a decrease beyond $Z_z = 100$ (Fm^{254}; Sm 58-2). The maximum at $Z_z = 98$ is accompanied by a sudden increase in the most probable mass number of heavy fission products and a discontinuity in the α-decay systematology (Gh 54-1, Gh 56-1). A new magic number ($N = 152$) is the end result (see ¶ 3.3).

In the case of a fixed target nucleus, $\overline{\overline{T_l + T_h}}$ is only very weakly dependent on excitation of the compound nucleus or bombardment energy (Wa 54-1, Sm 57-1). Apparently, $\overline{\overline{T_l + T_h}}$ decreases somewhat with increasing bombardment energy (Ju 49-1).

6. ANISOTROPY OF THE FISSION-FRAGMENT EMISSION

6.1. Introduction

The fission fragments do not fly apart isotropically if the symmetry axes of the splitting nuclei are oriented nonrandomly to the direction of bombardment at certain angles. Such nonrandom orientations can be achieved by orienting the target nuclei in appropriate chemical combinations at very low temperatures (Ro 57-1) or by means of changes to which the angular-momentum directions of the compound nuclei are subjected (as a result of the orbital-angular momentum of the bombarding particles contained in them).

If ϕ is the angle between the incident particle and the direction of flight of the fission product in the center-of-mass system of the splitting nucleus, the distribution of the fission products with respect to ϕ (the angular distribution) can be given by $a + b \cos^2\phi + c \cos^4\phi$ or $a + b \sin^2\phi + c \sin^4\phi$, with non-negative a and b. In general, the fission fragments are emitted nonrandomly at $\phi = 0$ in the first distribution and at $\phi = 90$ deg in the second. Frequently, the distributions with $c = 0$ are approximated with sufficient exactness; then, b/a serves as a measure of the anisotropy. Otherwise, the measure of the anisotropy is the number L (0 deg) of the fission fragments emitted at $\phi = 0$, divided by the number L (90 deg) of the fission fragments emitted at $\phi = 90$ deg, or some similar relationship.

In the laboratory system, the angle between the incident particle and the direction of the fission fragment is measured. This angle is now

considerably different from ϕ at higher bombardment energies. Sometimes the angle projected on a plane (photoplate) is used (Lo 55-1, Pe 55-1, Os 56-1, Ba 57-1, Ba 58-1). Refinements such as the above need not be considered in the following, since here the results are generally discussed only qualitatively. For quantitative comparisons with theories, extremely exact measurements are necessary (Co 58-2), especially in angular distributions, and the above-mentioned refinements can be significant.

Table 6.1 shows a survey of the measurements which have been made.

6.2. Photofission

6.2.1. Dependence of angular distribution of target nucleus and maximum photon energy.

The preferred emission angle (if any anisotropy exists at all) is ϕ = 90 deg. The angular distribution can be approximated by $a + b \sin^2\phi + c \sin^4\phi$ (Re 55-1, Ba 57-1, Ba 58-1); some authors are content with this distribution, with c = 0 (Wi 56-1, Fa 58-2, Ka 58-1, Co 59-1). The cause of the discrepancies which arise because of this is not quite clear; only part of them can be explained by underestimation of the statistical measurement fluctuation (Fa 58-2).

Anisotropy was observed in the even-even target nuclei of Th^{230}, Th^{232}, U^{238} but not in the even-odd and odd-even nuclei of U^{233}, U^{235}, Np^{237}, Pu^{239}, and Am^{241}.

The anisotropy decreases with increasing maximum photon energy E_e and disappears entirely when $E_e \simeq 16$ MeV (Fig. 6.21).

This is precisely the qualitative theoretical expectation if electrical dipole absorption ($l = 1$) is assumed (Bo 56-1, St 56-3). The even-even compound nucleus, then, has the angular momentum $I_z = 1$ in the direction of the photon ray. For the lowest levels of the nucleus at the saddle point of the fission, the projection of I_z onto the nuclear symmetry axis has the quantum number $K = 0$; this means that the symmetry axis is nonrandomly perpendicular to the direction of bombardment, from which the preferred emission angle for the fission fragments, $\phi = 90$ deg, follows. Further analysis will also result in the observed distribution $a + b \sin^2\phi$.

The levels with $K = 1$ in the even-even nucleus are about 1 MeV higher than those with $K = 0$. Only when E_e becomes correspondingly higher does the nonrandom direction $\phi = 0$ demanded by $K = 1$ enter the competition and reduce the anisotropy. With even higher E_e, none of the channels will be nonrandom any longer, and the anisotropy must disappear.

An even-odd or even-even compound nucleus can have different I_z, and the levels corresponding to the various K are

denser (closer together). Therefore, even with the smallest possible E_e, the fission will proceed through more than one channel; no anisotropy will therefore be achieved (Bo 56-1).

The term c $\sin^4\phi$ in the angular distribution denotes noticeable electrical quadrupole absorption (Ba 57-1), which appears strongest at E_γ = 7.5 MeV (Ba 58-1). However, the electrical dipole absorption always dominates.

6.22. Dependence of the angular distribution on the fission ratio A_h/A_l.

Thus far, the anisotropy was assumed to be averaged over all A_h/A_l. If we consider it as a function of A_h/A_l, we find that the anisotropy nearly disappears in symmetrical fission and increases strongly only as A_h/A_l increases (Wi 56-1). The significance of this is (St 56-3, Co 58-2, Ha 58-1, Ha 58-2) that compound or residual nuclei with small excitation, which, according to ¶ 6.21, split particularly anisotropically, also split less symmetrically than nuclei with greater excitation (¶ 4.221).

6.3 Thermal Fission of Oriented Nuclei

The thermal fission of oriented U^{233} nuclei leads to a weakly anisotropic fission-fragment emission, about which only provisional results are available (Ro 57-1, Ro 58-2). Orientation is effected by means of electrical

quadrupole coupling in crystals of $UO_2Rb(NO_3)_3$ at temperatures of about 1°K. According to theory, such anisotropy is to be expected, because in thermal fission only a few channels with specified angular-momentum quantum numbers I_z and K are available (Bo 56-1, Ro 58-2).

6.4 Fission by Neutrons With Energies 0.4 MeV $\lesssim E_n \lesssim$ 10 MeV

In the case of even-even target nuclei with a neutron threshold energy $E_n^h > 0$ (Th^{232}, U^{238}), ϕ = 90 deg is the preferred emission angle in the region in which the fission cross-section σ_f rises to the first plateau (¶ 1.32). For higher E_n, the preferred angle changes to $\phi = 0$; the amount of anisotropy fluctuates as a function of E_n (Fig. 6.4). Maximum amounts of anisotropy coincide with increases in $\sigma_f(E_n)$; i.e., they apparently occur when new fission channels become available (¶ 1.321). This is particularly apparent as $\sigma_f(E_n)$ rises to the second plateau (¶ 1.33).

It appears clear that a tendency toward small projections of the compound-nucleus angular momentum I_z exists in the impulse direction; this tendency will be proportionately greater as the orbital-angular momentum (perpendicular to the bombardment direction) of the bombarding particles increases and as the compound-nucleus angular momentum I_t decreases. A further tendency toward small projections K of I_z toward the symmetry axis of the nucleus (Bo 56-1, St 57-2), that is, in the direction of the fission-fragment emission, then leads to the preferred $\phi = 0$ for this emission. The observed angular distribution, too, follows on the basis of the above and of

further statistical analyses (St 57-2). The preferred direction $\phi = 0$ will be especially pronounced when a specific channel with small K makes a particularly strong contribution, as appears to be the case in the increase of $\sigma_f(E_n)$(Bo 56-1). The emission angle $\phi = 90$ deg in the region of the neutron threshold energy can be explained by appropriate corollary assumptions about K and l (l = 3)(Wi 56-2).

For even-odd target nuclei (U^{233}, U^{235}, Pu^{239}), $\phi = 0$ is always the direction of preferred emission (for $E_n > 0.4$ MeV). Here, too, the anisotropy fluctuates as a function of E_n, but it remains smaller (under about 1.3) than in the case of even-even target nuclei (Br 55-1; further provisional results in Bl 59-1, He 59-1, La 59-2). A maximum of anisotropy again appears to point to a new fission channel (La 59-2). The smaller amounts of anisotropy are understandable, because more channels are available and because the target nuclei do not have the angular momentum $I_t = 0$ (see above). However, the amount of I_t (U^{233}: 5/2; U^{235}: 7/2; Pu^{239}: 1/2) does not appear to affect the magnitude of the anisotropy systematically (He 59-1).

With E_n as high as perhaps 10 MeV, theory leads us to expect further anisotropy maxima in the case of even-even and even-odd nuclei if the reactions (n, 2nf), (n, 3nf), etc., become possible (Ha 58-2). Measurements in this energy region (He 56-1, Bl 59-1) are still not sufficiently numerous to permit clear recognition of maxima. However, here, too, the average anisotropy is smaller for even-odd nuclei than for even-even nuclei. This appears to be based, at least partially, on the various fission

probabilities: In the even-odd nuclei U^{233} and Pu^{239} (Bl 59-1), the reaction (n, f) is quite predominant over (n, nf), (n, 2nf), etc., so that highly excited compound nuclei split. This makes possible large K and thus requires smaller anisotropies (Ha 58-2; see above).

6.5 Fission by Particles With Energies E > 10 MeV

6.51. General

With particle energies of more than about 10 MeV, the fission fragments are almost always emitted anisotropically. The direction of preferred emission for 10 MeV $\lesssim E \lesssim$ 50 MeV is $\phi = 0$; the angular distribution has the form $a + b \cos^2\phi + c \cos^4\phi$ (Br 54-1, Br 55-1, Co 58-2). With particle energies of about 100 MeV, the emission angle can be changed to $\phi = 90$ deg; the angular distribution, in this case, can be represented by $a + b \sin^2\phi$; otherwise, by $a + b \cos^2\phi$ (Po 57-2, Wo 57-1). (a and b are always non-negative.)

The dependence of the anisotropy on the angular momentum of the target nucleus is insignificant compared to the dependence on Z^2/A of the compound nucleus (see ¶ 6.4., conclusion), should the latter be formed.

6.52. Dependence of the angular distribution on the target nucleus, the compound nucleus, and the excitation of the latter.

For a fixed bombarding particle of fixed energy, the anisotropy generally decreases noticeably as Z_z^2/A_z

increases (for neutrons: Br 54-1, Pr 58-3; for protons, deuterons, and α-particles: Co 58-2; for protons of very high energies: Po 57-2; for C^{12}-nuclei: Po 59-1). Figure 6.52, for example, shows anisotropy for the fission of seven target nuclei by deuterons and α-particles as a function of Z_z^2/A_z. The curves are quite smooth, even though the angular momentum I_t of the target nuclei fluctuates within broad limits. The anisotropy does not appear to depend intrinsically on I_t (Co 58-2, Pr 58-3). More detailed arguments (elimination of the dependence on Z_z^2/A_z and comparison of I_t and the transferred orbital-angular momentum l) reinforce this conclusion (Co 58-2).

The relationship between the anisotropy and the parameter Z_z^2/A_z of the liquid drop model appears unclear at first. However, it becomes understandable if the possibility of neutron emission before fission is considered (Co 58-2, Ha 58-1, Ha 58-2, see ¶ 6.4, conclusion). For excitation barely above the activation energy, the anisotropy decreases with increasing excitation U_z (Fig. 6.4). The high anisotropy at small Z_z^2/A_z can now come about in the following manner: small Z_z^2/A_z indicate great probability of neutron emission; from the latter, a residual nucleus with a smaller excitation is formed; this excitation, in

turn (when the residual nucleus is split), leads to high anisotropy. In the reactions Ra^{226} + d and Bi^{209} + α, light residual nuclei are created, for which the above arguments are not valid without modification (Ha 58-2).

6.53. Dependence of angular distribution on energy, angle, and orbital angular momentum of the bombarding particles.

For a fixed target nucleus, the anisotropy increases slowly, and generally smoothly, with increasing energy E of a fixed bombarding particle (Br 55-1, He 56-1, Co 58-2). This is connected with the fact that, on the average, particles of higher energy also transmit a higher orbital angular momentum (see below). Theory (Ha 58-2) leads us to expect maxima of anisotropy beyond this, as they were observed with smaller E (¶ 6.4), if, after the emission of an additional neutron, another fission possibility presents itself. Thus far, the measured data are so sparse that the possibility that further maxima might be found appears likely.

If, for a fixed target nucleus, the bombarding particle is varied, the anisotropy increases with increasing particle mass if E is fixed (Figure 6.52). This is probably the case because particles with greater mass can transmit a greater orbital angular momentum. With increasing transmitted orbital angular momentum, the anisotropy increases considerably.

The fission of the compound nucleus Pu^{239} yields L(0°)/ L(90°) = 1.19 or 1.38, depending upon whether it was created by Np^{237} + d or by U^{235} + α; E_d and E_α are selected in such a way that the compound-nucleus excitation is equal in both cases (Co 58-2). In this example, α-particles transmit about 1.7 times more orbital-angular momentum than deuterons. The increase in anisotropy with increasing orbital angular momentum l is understandable, because fewer directions are available to the angular momentum I_z of the compound nucleus if l is large (St 56-3).

At bombardment energies E > 100 MeV, the fission fragments are generally no longer emitted nonrandomly in or against the bombardment direction (at ϕ = 0) but rather, nonrandomly at ϕ = 90 deg. Figure 6.53 shows this for the fission of U^{238} by protons (Lo 55-1, Pe 55-1, Me 58-1); the same is true for the fission of U^{238} by fast neutrons (Os 56-1) and of Ta by 450-MeV protons (Po 57-2). However, in the fission of Bi by 450-MeV protons, ϕ = 0 is (as otherwise at small E) the preferred emission angle.

The generally anomalous anisotropy (preferred emission angle ϕ = 90 deg) at E $\gtrsim$ 100 MeV stems from the fact that with such high E, compound nuclei are no longer formed; instead, the bombarding particle releases a nucleon cascade (¶ 1.1). The bombarding particle essentially retains its

direction of flight; the impacted nucleons, on the other hand, attain nonrandom velocities perpendicular to the bombardment direction and only very low kinetic energies. These nucleons are again partially absorbed by the nucleus and are capable of exciting it to fission, during which the fission fragments are emitted nonrandomly in the direction of the absorbed particles, as was observed in the case of weakly excited compound nuclei. This means that the fission fragments fly off nonrandomly perpendicular to the direction of the primary bombarding particles (Ha 59-1). A semi-quantitative observation yields an approximation of the noted angular distribution $a + b \sin^2\phi$.

In essence, it should be the residual nuclei with <u>small</u> excitation U_k that remain after the cascade which are responsible for the high anisotropies (see ¶ 6.4). Thus, the divergent behavior of Bi might be explained by the fact that with such light target nuclei, fissions are not possible with small excitations (Ha 59-1). This explanation appears unsatisfactory in view of the different kind of behavior of Ta. Besides, it was found that (for $U_k \geq 50$ MeV) the anisotropy appeared to increase; if only weakly, with increasing U_k (Lo 55-1, Pe 55-1, Os 56-1).

6.54. Dependence of the angular distribution on the fission ratio A_h/A_l.

To this point, the anisotropy was understood to be averaged over all A_h/A_l. If it is considered as the function of A_h/A_l, the anisotropy disappears during symmetrical fission and increases only as A_h/A_l increases (fission by neutrons: Pr 58-2, by protons: Co 54-1, Co 55-1, Me 58-1; Fig. 6.54). This law appears to be valid even for the fission of Ta with 450-MeV protons, although the data are very inexact (Po 57-2). The law also holds for photofission; the interpretation is the same (¶ 6.22).

The transition of the preferred emission angle $\phi = 0$ to $\phi = 90$ deg for fission by neutrons and protons with energies of about 100 MeV occurs at higher E for $A_h/A_l \simeq 1$ than it does for $A_h/A_l > 1$ (Me 58-1). This, too, appears to be connected with the different excitations of splitting nuclei (see ¶ 6.52, conclusion).

In general, no preferred emission angle was determined for heavy fission fragments (as opposed to light fission fragments). Only in the fission on Np^{237} by neutrons were considerably more heavy fission products discovered for $\phi = 0$ (in the direction of the bombarding particles) than for $\phi = 180$ deg (Br 55-1).

7. NUCLEAR CHARGE OF THE FISSION PRODUCTS

7.1. Introduction

The nuclear charge of a fission product is interpreted to be its nuclear charge before the first β-decay (¶ 4.1). In the appendix to ¶ 4.1, a few new concepts are introduced.

The independent yield, divided by the associated chain yield, is designated as the specific independent yield. It is customary to base its computation on a chain yield which comes from a smoothed mass distribution (without microstructure).

For a fixed mass number A, the specific independent yield as a function of nuclear charge Z yields the charge distribution for this fixed mass number. The sum of all the independent outputs for a fixed Z (neglecting A), written as a function of Z, is the distribution of all fission products with respect to their nuclear charge.

The cumulative yield of a nuclide is the sum of the independent yield of this nuclide as a fission product and the cumulative yield of its β-decay predecessor (recursive definition). The specific cumulative yield is the cumulative yield divided by the associated chain yield from a smoothed mass distribution. Shielded nuclides are those which could not have been created through β-decay. Their cumulative yield, therefore, is equal to their independent yield.

7.2. Measured Results

7.21. Independent yields.

An exact determination of charge distribution presupposes the measurement of independent yields. Such measurements are very difficult to make for thermal and spontaneous fissions, because the half lives of the fission product often amount to mere seconds. Therefore, the measured data (Table 7.21-1) are very limited. Frequently, only upper limits can be given.

In fission by faster particles, independent yields can be determined more easily, because the fission products, on the average, are more stable against β-decay. The reason for this is that fission at high energies is connected with the emission of a greater number of neutrons (¶ 1.43). Therefore, the specific independent yields do not fluctuate in such broad limits as they do in thermal fission. Table 7.21.2 shows studies in which independent yields have been determined.

7.22. Width of the charge distribution for a fixed mass number.

If we are content merely to determine the width of a charge distribution, a way other than the measurement of independent yields is available. Since the mean total charge of a fission product depends upon its nuclear charge, the width of a charge distribution can be determined through deflection

in a magnetic field: in the thermal fission of U^{235}, the charge distribution for the mass number A = 97 is a gaussian curve with a width of 2.4 ±0.5 (Co 58-1).

The charge distribution, which was constructed from specific independent yields in thermal and spontaneous fission, has a width of about 2.2 (Eq. 51-1; see ¶ 7.41). The statistical theory of fission (Fo 56-1), on the other hand, reports a width of only 1.2. The width of the charge distribution (¶ 7.42) increases with increasing bombardment energy.

7.23. Width of the distribution of all fission products with respect to their nuclear charge.

The distribution (in thermal fission) has two maxima, as does the mass distribution. The width of the maxima can be estimated, using Moseley's law, from the width of the maxima of the X-ray-K spectrum of the fission products (see ¶ 8.32). The width of the maxima (for thermal fission of U^{235}) was found to be about 14.5% for the light fission-product group (most probable Z: 40) and 17% for the heavy group (most probable Z: 56) (Sk 59-1).

7.3. Postulate for the Charge Distribution for Fixed Mass Number

It is not possible to construct a charge distribution for every mass number A from the few known independent yields. Therefore, we postulate that the charge-distribution curves for all A can be made to coincide if $Z - \langle Z \rangle$

can be entered on the abscissa instead of Z, where $\langle Z \rangle$ is the charge number of the appropriate isobars which will most probably appear (not necessarily the whole charge number). This postulate is in agreement with statistical theory (Fo 56-1) and has given good results. In addition, it is usually assumed that the charge distribution is independent of the target nucleus if the excitations of the splitting nuclei are all comparable; this assumption, too, has been proven to be a good one.

The following postulates were suggested for the determination of $\langle Z \rangle$. They are either empirical or are based on theoretical considerations. The (not necessarily whole) charge number of the (hypothetically) most stable isobar for the A under consideration has been designated by Z'.

a. The postulate of regular charge distribution (Eq. 51-1+) is based on the liquid drop model. The splitting nucleus and the fission fragments should have equal charge densities. The β-decay chains, then, are longer for light fission products than for heavy ones in thermal fission.

b. The postulate of equal decay-chain lengths (Eq. 51-1) requires equal lengths of the β-decay chain for all complementary (i.e., created in <u>one</u> fission) fission products:

$$Z'(A_l) - \langle Z \rangle (A_l) = Z'(A_s) - \langle Z \rangle (A_s) \qquad (7.3)$$

Different assumptions about Z' lead to different $\langle Z \rangle$ (℞ 7.4).

c. The postulate of inhomogeneous charge distribution (Pr 47-1) states that the Coulomb repulsion of the nuclear charges leads

to charge transpositions in which a greater mean charge density results for the light fission fragment than for the heavy fission fragment.

d. The postulate of minimum potential energy (Wa 48-1, Wa 49-1) requires such a distribution of the charge among the fission fragments that the sum of the Coulomb and binding energies of the fission fragments has a minimum. The resulting β-decay chains are shorter for the light fission products than for the heavy ones.

e. The postulate of the greatest liberating energy (Ke 56-1) requires a minimum for the sum of the two fission-fragment masses (computed as in Ku 55-2).

7.4. Proof of the Postulates

7.41. Thermal and spontaneous fission.

Postulates b and e have proved to be usable. In agreement with Co 58-1, the charge distribution for fixed mass numbers is generally nearly a gaussian curve. Its width is approximately 2.2 (Eq. 51-1; see ¶ 7.22).

In postulate b, various $\langle Z \rangle$ result, depending upon the choice of Z'. Originally (Eq. 51-1), a smooth function Z' (A) (Wa 44-1) was used; thus, $\langle Z \rangle$ (A) was also smooth. The charge distribution is shown in Fig. 7.41-1. Consideration of the shell effect leads to an unstable function Z' (A) (Co 53-1) and thus, to an unstable function $\langle Z \rangle$ (A) (Pa 53-1, Pa 56-1); the

dispersion of the measured points about the charge-distribution curve decreased (Fig. 7.41-2). A similarly narrow dispersion of the measured points resulted when mean values were taken for the unstable function Z' (A) in the region of magic numbers (St 56-2).

The basic purpose of postulate e is to allow for shell effects not only for Z' but also for $\langle Z \rangle$. On the basis of postulate e, two new independent yields (I^{128}, I^{130}) fit the charge-distribution curve better (Ke 56-1).

On the basis of newer data for the nuclear masses (Wa 55-2, Ca 57-1, Ha 57-1), the $\langle Z \rangle$ were recomputed according to postulates b and e (Gr 57-2). Postulate b was confirmed quite satisfactorily; postulate e resulted in a smaller influence of closed shells on $\langle Z \rangle$ than in Ke 56-1 and yielded an unsymmetrical charge distribution.

Because of the lack of clarity concerning the most suitable method for calculating the function $\langle Z \rangle$(A) from postulate b, the $\langle Z \rangle$ for U^{235} were also determined empirically (Wa 58-1): according to Eq. 51-1, Pa 56-1, and St 56-2, the $\langle Z \rangle$ (A) lead essentially to the same charge-distribution curve. The latter was retained, and the $\langle Z \rangle$ were fixed in such a way that each measured independent yield lay precisely on the curve; measured cumulative yields (Table 7.21-1) were also taken into consideration. Figure 7.41-3 shows the function which was

thus obtained. It is essentially smooth, as is the one originally computed (Eq. 51-1).

7.42. Fission by bombarding particles with energies $E \gtrsim 5$ MeV.

Although postulates a and b have proved usable, they partially contradict the results.

Analysis of measured independent yields gives the following results: for bombardment energies $E < 15$ MeV, postulate b is effective. The charge distribution is nearly in the form of a gaussian curve (Fo 53-1, Wa 55-1, Al 57-1; compare Table 7.21-2 with these and the following references). In the region 15 MeV $\lesssim E \lesssim$ 50 MeV, none of the postulates is confirmed satisfactorily; if the data are matched to postulate a (Gi 56-1) or b (Fa 58-1), the charge distribution is no longer a gaussian curve. In general, postulate a has been satisfactory for $E \gtrsim 75$ MeV (Go 49-1, Fo 55-1, Jo 55-1, Kr 55-1, La 57-2, Po 57-2). In the fission of Ta^{181}, postulate a appears valid according to Kr 55-1 and postulate b according to Po 57-2, Pa 58-3+.

A less direct method (Pa 58-3) for confirming the validity of the postulate is the Monte-Carlo computation of the total reaction and comparison of the computed ratio N/Z of the neutron and proton number of the fission product with experimentally determined N/Z (La 57-2, Pa 58-1). The Monte-Carlo

computation was accomplished using Do 58-1, Me 58-2, Me 58-3, and making a simple assumption about the dependence of $\overline{\Gamma}_n / \overline{\Gamma}_f$ on Z^2/A for the reaction $Th^{232} + p (E_p = 8$ MeV). and $U^{238} + p$ (E_p = 83 and 450 MeV). In each case, postulate b was found valid.

Figure 7.42 (Pa 58-1) shows the dependence of the charge distribution on bombardment energy E. As E increases, $\langle Z \rangle$ moves closer to Z', and the width of the curve increases (from 2.2 for E $\lesssim$ 25 MeV to 3.2). The displacement of the maximum is required by the number of emitted neutrons, which rises as E increases; $\overline{\nu}$ can be estimated from a charge distribution (Wa 58-2). The widening of the curves corresponds to the increasing number of possible splitting nuclei with different excitations if E increases (¶.1.44).

8. PROMPT NEUTRONS AND GAMMA RAYS

8.1. Introduction

The neutrons and gamma rays which are emitted no later than 5 x 10^{-8} sec after fission are designated as prompt. Delayed neutrons (Ke 58-1) and delayed gamma rays are emitted in connection with the β- delays and K- captures of the fission products. They are not treated in this paper. However, the number ν of the neutrons emitted per fission (¶ 8.21 and 8.23) by definition also contains the delayed neutrons. Since the latter amount to only 1% of the total neutrons (Ke 58-1), their contribution to ν (which is generally smaller than the measurement error) is not considered further.

In compound-nucleus excitations $U_Z > 10$ MeV, (n, nf)-reactions, and with higher U_Z even (n, 2nf)-reactions, etc., are possible (¶ 1.33). The neutrons emitted <u>before</u> fission are considered prompt by definition and are also contained in the number ν (¶ 8.212). Of course, certain statements (e.g., about angular relationships) do not apply to them (this will not be pointed out again in this paper). For $U_Z \gtrsim 20$ MeV, the fission is connected with the emission of even more numerous lighter particles, about the nature and time of whose origin no precise statements can be made (¶ 1.43). Hence,¶8 is applicable only to fission processes in which no compound-nucleus excitations higher than 20 MeV occur.

The upper limits, 10^{-13} sec (Er 57-1+) and 4 x 10^{-14} sec (Fr 52-1), have been determined experimentally (in the thermal fission of Pu^{239}) for the

times in which the major portion of the prompt neutrons is emitted. Gamma-radiation is emitted until about 10^{-5} sec after fission (because of isomeric transitions), but the energy of the radiation emitted between 5 x 10^{-8} and 10^{-5} sec after fission amounts to an average of only 5% of the energy of the prompt gamma-radiation (thermal fission of U^{235}, Ma 58-1).

Basically, prompt neutrons and gamma rays could be emitted from the splitting nucleus or from the fission fragments. In the following paragraphs, a number of experimental results are cited for neutrons, which can be explained by assuming emission from the fission fragments (¶ 8.22 and 8.24). These explanations are based on the assumption that the fission fragments have already attained their full velocity during the neutron emission, which means that the neutrons are emitted at least 10^{-20} sec after the separation of the fission fragments (Te 59-1). In the case of gamma-radiation, the experimental indications of fission-fragment origin are less numerous (¶ 8.32 and 8.33). It does not appear impossible that at least a portion of the radiation is emitted during the acceleration of the fission fragments (¶ 8.32, conclusion).

8.2. Prompt Neutrons

8.21. Mean number $\bar{\nu}$ of neutrons emitted per fission

8.211. Dependence of $\bar{\nu}$ on the compound nucleus in spontaneous and thermal fission. Table 8.211 lists the measured $\bar{\nu}$ for thermal and spontaneous fission processes. $\bar{\nu}$ increases with increasing mass number A_Z of the compound

nucleus. Systematic mathematical interrelationships in $\bar{\nu}$ can be expected only after conversion to equal compound-nucleus excitations U_z. With the aid of the results from ¶ 8.212, an extrapolation of $\bar{\nu}$ for thermal fission was made for $U_z = 0$, and $\bar{\nu}$ was then written as a function of A_z (Bo 58-3). The function is only very roughly linear. A computation, which is based on Eq. 5.1-4, on simple observations of energy using experimental results, and on a simplified distribution of the fission-product masses, yields separate curves $\bar{\nu}$ (A_z) for various nuclear charges Z_z, to which the experimentally determined points have a reasonably good fit (Bo 58-3). The simpler provisional computations (Ko 58-1) lead to the same results within the range of computation accuracy.

8.212. Dependence of $\bar{\nu}$ on bombardment energy. $\bar{\nu}$ was measured for the target nuclei U^{233}, U^{235}, and Pu^{239} at bombarding neutron energies E_n between 0.025 ev and 15 MeV for the target nuclei Th^{232}, U^{238}, Np^{237}, Pu^{240}, and Pu^{241} in narrower E_n regions. Le 58-1+ contains a comprehensive table of the measurement values; Table 8.212 gives additions to this table. Figure 8.212 shows $\bar{\nu}$ as a function of E_n for some nuclei.

For $E_n < 0$, too, $\bar{\nu}$ increases linearly with increasing E_n (spontaneous fission of the compound nucleus). This is to

be expected for $E_n \lesssim 5$ Mev [as long as no (n, nf)-reactions are possible] (Le 56-1+, Le 56-2, Te 57-1, Bo 58-3) if the bombardment energy affects only the excitation of the fission fragments but not their kinetic energy (¶ 5.1). However, $\bar{\nu}(E_n)$ continues to increase nearly linearly up to $E_n = 15$ MeV. The explanation for this rests upon the fact that with (n, nf)-reactions the excitation of the splitting nucleus is lower than that of the splitting compound nucleus with (n, f)-reactions. The fission fragments thus generally emit fewer neutrons with (n, nf)-reactions, and this nearly compensates for the emission of a neutron before fission (Bo 58-3, Le 58-1, Sm 58-3), because the neutron binding energies in the compound nucleus and the fission fragments are approximately equal and, with fixed excitations, $\bar{\nu}$ varies very little from nucleus to nucleus. Similar observations apply to $E_n \gtrsim 13$ MeV if (n, 2nf)-reactions have become possible.

It is in accord with the linear variation of $\bar{\nu}(E_n)$ that for 0.025 ev $\lesssim E_n \lesssim 0.5$ ev, $\bar{\nu}$ does not change measurably (Au 55-1, Ka 56-1, Sa 56-2, Bo 58-1).

8.213. <u>Dependence of $\bar{\nu}$ on the fission ratio A_h/A_l and on the mass number A of the emitting fission fragment.</u>

Experiments were performed with the thermal fission of U^{233} (Fr 54-1), the spontaneous fission of Cf^{252} (Hi 57-1, Bo 58-2, St 58-3, Wh 59-1), and the fission of U^{238} by deuterons (Su 57-1). Measurements of U^{233} are not always

in agreement with those of Cf^{252} (perhaps as a result of the smaller probability of provable neutrons).

Figure 8.213-1 shows the likelihood of neutron emission as a function of A_h/A_l for U^{233} separately, for the light and heavy fission fragments. The majority of the neutrons are emitted from the heaviest fission fragments of the light group and from the heaviest fission fragments of the heavy group. In the approximate region of the most probable A_h/A_l, the likelihood of emission has a broad maximum, as has been predicted in the statical theory (Fo 56-1). On the average, the light fission fragment emits 1.24 times more neutrons than the heavy one.

The number of neutrons emitted by a fission fragment was measured for Cf^{252} as a function of the mass number A (Wh 59-1). The results (Fig. 8.213-2) include the assumption that the neutrons are emitted isotropically in the center-of-mass system of the fission fragment. On the average, the light fission fragment emits 1.02 times more neutrons than the heavy one. The sudden change in the neutron number near $A_H/A_L = 1$ also occurs for U^{233}, according to Fig. 8.213-1. It indicates that the light fission fragment is excited to a much greater extent than the heavy one if fission is nearly symmetrical. The magic number N = 82 (A = 133 - 134) could contribute to this change which is not reflected in the

distribution of the fission-product masses (¶ 4). Of course, it might only be apparent; in that case, the assumption of isotropic neutron emission would have to be entirely false (Wh 59-1).

The function $\bar{\nu}$ (A_h/A_l) can be constructed from Fig. 8.213-2. Direct measurements give the best agreement (St 58-3). The curves $\bar{\nu}$ (A_h/A_l) in Hi 57-1 and Bo 58-2 have a somewhat different appearance (apparently as a result of lower measured results). The maximum of $\bar{\nu}$ at the most probable A_h/A_l which was observed for U^{233} is not yielded in the case of Cf^{252}; rather, $\bar{\nu}$ decreases in this region as A_h/A_l increases.

In the fission of U^{238} by deuterons, too, the number of neutrons emitted per fission decreases roughly with increasing A_h/A_l (Su 57-1, see Table 1.432).

8.214. Dependence of $\bar{\nu}$ on the total kinetic energy $T_l + T_h$ of the fission products. Figure 8.214 shows $\bar{\nu}$ as a function of $T_l + T_h$ for the spontaneous fission of Cf^{252} (according to St 58-3). The corresponding curves in Hi 57-1 and Bo 58-2 have a somewhat different appearance (apparently as a result of lower measured results).

In addition, $\bar{\nu}$ as a function of $T_l + T_h$ for various ranges of the fission ratio A_h/A_l and $\bar{\nu}$ as a function of A_h/A_l for various ranges of $T_l + T_h$ were also determined (Hi 57-1,

St 58-3). The results agreed in that they showed $\bar{\nu}$ to be a linear function of both arguments in the region of the most probable A_h/A_l and $T_l + T_h$.

$\partial\bar{\nu} / \left[\partial(T_l + T_h)\right]$ can be estimated theoretically. According to Eq. 5.1-3, a decrease in $T_l + T_h$ must result in an increase of the entire fission-fragment excitation $U_L + U_H$ and, hence, a larger $\bar{\nu}$, since the sum F of kinetic and excitation energy for a given A_h/A_l is fixed by Eq. 5.1-4 (except for small fluctuations caused by different fission-fragment nuclear charges). Assuming $U_L + U_H$ to be distributed evenly over all nucleons of the fission fragments, the evaporation theory yields a (negative) value for $\partial\bar{\nu} / \left[\partial(T_l + T_h)\right]$ (Le 57-1), around which the experimentally determined values (Hi 57-1, St 58-3) also lie. In the thermal fission of U^{233} (Fr 54-1), on the other hand, the differential quotient was found to be approximately zero. This would mean that $\bar{\nu}$ can depend on $T_l + T_h$ only through A_h/A_l, and thus, (Eq. 5.1-3) on the fission-fragment excitation $U_L + U_H$.

8.22. Energy spectrum

Table 8.22 supplies information about measurements of the distribution of prompt neutrons with respect to their energy T_n (their energy spectrum in the laboratory system). The spectra for the various fission processes are

very similar; the mean energy $\overline{T}_n$ increases with increasing Z_z^2/A_z (Ko 58-3).

The measured spectra can be reproduced very well within the experimental accuracy, by two different distributions. The first is the Maxwell distribution

$$N_n(T_n) = \frac{2}{\sqrt{\pi}\, a^{3/2}} \sqrt{T_n} e^{-\frac{T_n}{a}} \qquad (8.22\text{-}1)$$

with a parameter a (Bl 43-1, Te 59-1). The second distribution

$$N_n(T_n) = f(b,c)\, e^{-\frac{T_n}{b}} \sinh \sqrt{cT_n} \qquad (8.22\text{-}2)$$

with two parameters b and c (Wa 52-1, Er 57-1+) follows, if isotropic emission with a Maxwell distribution of neutron energies is assumed in the center-of-mass system of the fission fragment. Figure 8.22 shows both distributions, together with experimental data for Cf^{252}. Some of the values of $\overline{T}_n$ in Table 8.22 are averaged from values yielded by Eqs. 8.22-1 and -2.

The evaporation theory (Bl 52-2) based on the statistical nuclear model, assuming isotropic neutron evaporation in the fission-fragment center-of-mass system, does not yield a Maxwell distribution of the neutron energy ϵ_n in this system but rather (with some simplifications), the distribution

$$N_n(\epsilon_n) \sim \epsilon_n e^{-\frac{\epsilon_n}{Q}} \qquad (8.22\text{-}3)$$

in which Q is the so-called temperature of the fission fragments <u>after</u> the emission of <u>one</u> neutron (Bl 52-2). The resulting distribution of T_n with fixed Q (Fe 42-1, Fe 51-1) does not parallel the measured spectrum (Te 59-1). Therefore, numerical calculations of the T_n distribution based on the evaporation theory (Table 8.22) should come from a distribution of Q, which, in turn, is related to the distribution of the fission-fragment excitations U_L and U_H (as was the case in Te 59-1). The results of such calculations differ only slightly from the Maxwell T_n distribution (which has been confirmed experimentally)(Te 59-1). This result does not change if the assumption of isotropic neutron emission is neglected; in an isotropic neutron emission, the T_n-distribution is even more similar to a Maxwell distribution.

The mean nuclear temperatures $\overline{Q}$ (Table 8.22) were determined from

$$\overline{T}_n = 0.78 \text{ MeV} + 2\overline{Q} \qquad (8.22\text{-}4)$$

This equation (Te 59-1) is based upon numerous measurements of energy magnitudes and on the spectrum of Eq. 8.22-3.

Statistical theory yields only a very slight increase in $\overline{T}_n$ with increasing excitation U_z of a fixed compound nucleus (Ba 57-2, Le 57-1); i.e., $d\overline{T}_n/dU_z \simeq 0.046/\sqrt{\nu + 1}$ (Te 59-1). So far, this slight increase could not be confirmed experimentally (Ko 58-1).

8.23. Probable emission of exactly ν neutrons per fission.

Table 8.23 shows the measured results of the probable emission of exactly ν neutrons per fission. Semi-empirical computations of this probable emission were carried out by two different methods.

In one method, the total excitation $U_L + U_H$ of the fission fragments and their distribution over Eqs. 5.1-3 and -4 is computed from the measured distribution of the kinetic energy $T_l + T_h$ (¶ 5.5); using the evaporation theory, the distribution of $U_L + U_H$ yields the distribution of ν; that is, the probable emission being sought (Co 56-1, Le 56-2). The calculated probabilities are in good agreement with the measured ones, as is shown in Fig. 8.23.

In the other (simpler) method, a gaussian distribution of $U_L + U_H$ is postulated, with a width which is proportional to the average value of $B_n + T_n$ (binding energy and kinetic energy of an emitted neutron). If 1.08 is selected as the proportionality factor (except for Cf^{252}, in which case it is 1.21), the distribution of ν which results from the distribution of $U_L + U_H$ is a good reproduction of the measured results (Te 57-1).

8.24. Angular relationships

8.241. Angular relationships between the directions of flight of the fission fragments and the neutrons. In the

experimental system, measured angular distributions for the emitted neutrons with respect to the direction of flight of the light fission fragments can indicate (although not always conclusively) whether or not the neutrons in the center-of-mass system of the fission fragment are emitted isotropically and whether the two fission fragments usually emit the same or different numbers of neutrons. The angular distribution was measured for the thermal fission of U^{233} (Fr 52-1), U^{235} (Fr 52-1, Ra 58-1), and Pu^{239} (Fr 52-1) and for the spontaneous fission of Cf^{252} (Fn 59-2).

For confirmation, the measured angular distribution is compared with a computed one (Fr 52-1, Ra 58-1, Te 59-1). In the computations, isotropic neutron emission and the energy spectrum of Eq. 8.22-3 (without a fixed nuclear temperature) were assumed in the fission-fragment center-of-mass system. The angular distribution was obtained as a function of the quotient of the numbers of neutrons from light and heavy fission fragments. In Fr 52-1, calculated and measured angular distributions agree, if it is assumed that the light fission fragment emits approximately 1.3 times as many neutrons as the heavy one. Other authors obtain 1.2 (Ra 58-1), 1.1 to 1.2 (Te 59-1, using the

measured results of Fr 52-1), or 1.25 (Sn 59-2) for this factor. A few somewhat deviating values of this factor are found in other experiments (¶ 8.213).

In Ra 58-1, calculated and measured angular distributions for small angles do not agree at any value of the above-mentioned factor. One must therefore conclude that the neutron emission in the direction of flight of the fission fragment (in the fission-fragment center-of-mass system) is nonrandom; i.e., the neutron emission is not isotropic. A possible explanation for this nonrandom direction is that the neutrons are emitted immediately after the separation of the contracted deformed fission fragments (Hi 53-1, St 59-1). However, there is no experimental proof either for or against isotropic emission (Te 59-1).

8.242. Angular relationships between prompt neutrons. Measurements of the angular distribution between two neutrons generated in the same act of fission should be capable of supplying information about whether pairs of neutrons stem from the same nuclear fragment or from different ones. Experiments were made with the fission of U^{235} (Be 48-1) and natural uranium (Sk 56-1) by slow neutrons; the measured angular distributions are contradictory. In Be 48-1, the distribution is nearly constant

from 0 to 90 deg and then increases by a factor of two up to 180 deg; to be sure, the measured values are somewhat uncertain for small angles (Sk 56-1). In Sk 56-1, the distribution is symmetrical, with a minimum at 90 deg. It may be concluded from the first distribution that twice as many neutron pairs are emitted by fission fragments stemming from different acts of fission than by those generated in the same act (Be 48-1), and from the second distribution (using the results from ¶ 8.241), that neutron pairs can stem from fission fragments generated in the same and in different acts of fission with equal probability (Sk 56-1).

8.243. Angular relationships between the directions of flight of the bombarding particles and of the neutrons. The angular distribution between the directions of flight of the bombarding particles and the prompt neutrons was calculated for the fission of U^{238} by neutrons with energies between 1 and 10 MeV (Ba 57-2). The directions of flight of the fission fragments were determined by means of a simplified angular distribution, according to Br 55-1 (¶ 6.5); for the prompt neutrons, isotropic evaporation from the fission fragments in the fission-fragment center-of-mass system was assumed. A nonrandom direction of the neutron velocities in the direction of the bombarding neutrons resulted in experimental system.

8.3. Prompt Gamma-Radiation

8.31. Average number of prompt gamma rays emitted per fission.

Table 8.3 shows the measured values for the mean number $\overline{N}_\gamma$ of the gamma rays emitted per fission. For Cf^{252}, $\overline{N}_\gamma$ was investigated as a function of the total kinetic energy $T_l + T_h$ of the fission products and of the fission ratio A_h/A_l (Mi 58-1). $\overline{N}_\gamma$ decreases linearly with increasing $T_l + T_h$, but the dependence is much weaker than the corresponding one for $\overline{\nu}$ (¶ 8.214). As a function of A_h/A_l, $\overline{N}_\gamma$ shows a minimum at $A_h/A_l \simeq 1.1$; a further minimum at $A_h/A_l \simeq 1.86$ is indicated. This relationship is attributed to the shell effect: at $A_h/A_l = 1.1$, the heavy fission fragment has slightly more than 50 protons and 82 neutrons; at $A_h/A_l = 1.86$, the light fission fragment has little more than 50 neutrons.

8.32. Energy spectrum.

Figure 8.32 shows the measured spectra of prompt gamma-radiation for the thermal fission of U^{235} (0.3 MeV $\leq T_\gamma \leq$ 8 MeV, Ma 58-1) and the spontaneous fission of Cf^{252} (0.25 MeV $\leq T_\gamma \leq$ 8 MeV, Sm 56-2). Additional measurements of the spectrum for Cf^{252} are available for limited T_γ ranges (Mi 58-1, Bo 58-2).

In the 100-kev $\leq T_\gamma \leq$ 800-kev range, eight distinct lines were found (in the thermal fission of U^{235}) (Sk 57-1, Vo 57-1). For the radiation with $T_\gamma \leq$ 250 kev, these lines were shown to originate in the fission fragments (Sk 57-1; see ¶ 8.1) by the geometric arrangement of the detection apparatus. The opinion has been expressed (Pr 58-4) that the lines could also be created in different fission fragments through the superposition of γ-transitions of nearly equal energy.

Radiation maxima at 16 and 31 kev (Sk 59-1) and, according to another source (Le 58-2 +), at 18 and 32 kev, were interpreted as X-ray K-radiation and maxima at 2.1 and 3.6 kev (Le 58-2 +) as L-radiation. The maxima in the spectrum at 16 and 31 kev are too broad to be considered lines. They appeared to be created from fission fragments of the light group (16 kev) and the heavy group (31 kev) through the superposition of K-radiation (Sk 59-1; see ¶. 7.23). Corresponding maxima exist in the thermal fission of U^{233} and Pu^{239} (Sk 59-1).

The prompt gamma spectrum emitted during the fission of U^{235} was measured as a function of the bombardment energy. At neutron energies of 0.025 ev, 2.8 MeV, and 14.7 MeV, the spectra vary only within ±15% (Pr 58-4).

The dependence of the mean energy $\overline{T}_\gamma$ of a gamma ray upon the total kinetic energy $T_l + T_h$ of the fission products is slight; as a function of the fission ratio A_h/A_l, $\overline{T}_\gamma$ appears to have maxima where N_γ (¶ 8.31) shows minima (Mi 58-1).

Table 8.3 lists measured and calculated values for the total energy $\overline{\Sigma T}_\gamma$ liberated in the form of gamma-radiation during a fission. The calculations are based on the assumption that the gamma-radiation is emitted by the fission fragments only when the emission of neutrons is no longer possible in terms of energy; the other assumptions are the same as those for the calculation of the spectrum of prompt neutrons (Le 56-2, Le 57-1; see ¶ 8.22). The large discrepancy between calculated and measured values of $\overline{\Sigma T}_\gamma$ indicates that, actually, the gamma-radiation is not emitted only after the end of the neutron emission (Te 59-1). This could be due to the very strong electromagnetic fields which appear during the acceleration of the fission fragments immediately after their separation (Te 59-1).

8.33. <u>Angular relationships between the directions of flight of the fission fragments and the gamma rays</u>.

Measured angular distributions for the emitted gamma rays with respect to the direction of flight of the fission

fragments in the laboratory system can give an indication of whether or not the gamma rays in the fission-fragment center-of-mass system are emitted isotropically. Measurements of thermally split U^{235} and Pu^{239} showed that the gamma rays are emitted anisotropically by the fission fragments, with very weak nonrandom direction in and against the direction of flight of the fission fragments (Le 58-2 +). A brief note (Hu 56-2) indicates that (in the case of U^{235}) more photons are emitted in the direction of the light fission fragment than in the direction of the heavy one.

REFERENCES

Introductory Remarks

The abbreviations for the references are composed of the first two letters of the last name of the senior author. The last two numbers of the year in which the work (in several cases, the first one listed) has appeared, and a serial number.

In the references themselves, the following abbreviations, which are not always in general use, are employed.

AE	Atomnaya Energiya
AEC-tr	Russian publication translated by the Atomic Energy Commission (USA)
AECD AECU ANL BNL CF CP HW LA LADC NYO ORNL ORO TID UCRL	Research report of the Atomic Energy Commission (USA)
AERE BR	Research report of the Atomic Energy Research Establishment (Harwell, Great Britain)
AERE-Lib/Trans	Russian publication translated by the Atomic Energy Research Establishment
Atomenergie	Conference of the USSR Academy of Sciences on the Peaceful Uses of Atomic Energy Berlin: Akademie-Verlag.

REFERENCES (Cont'd)

Conf. Acad. Sci. USSR	Conference of the Academy of Sciences of the USSR on the Peaceful Uses of Atomic Energy. Atomic Energy Commission (USA)
CRC(AECL) CRP(AECL)	Research report of the Atomic Energy of Canada Ltd.
JETP	Soviet Physics (JETP)
NP	Foreign reports obtainable through the Atomic Energy Commission (USA)
NNES	National Nuclear Energy Series. New York: McGraw-Hill.
PNF	Physics of Nuclear Fission, Supplement No. 1 of the Soviet Journal Atomnaya Energiya. London: Pergamon Press.
PR	The Physical Review
PUAE	Proceedings of the International Conference on the Peaceful Uses of Atomic Energy. New York: United Nations 1956. Proceedings of the Second United Nations International Conference on the Peaceful Uses of Atomic Energy, United Nations, Geneva, 1958.
Sessiya Akad. Nauk SSSR	Sessiya Akademii Nauk SSSR po mirnomu ispolzovaniyu atomnoi energii. Moskau: Verlag der Akademie der Wissenschaften der UdSSR.
SJAE	Soviet Journal of Atomic Energy
ZETF	Zhurnal eksperimentalnoi i teoreticheskoi fisiki

Aa 57-1 P. Aagaard, G. Andersson, J.O. Burgman u. A.C. Pappas: J. Inorg. Nucl. Chem. **5**, 105.

Al 50-1 K.W. Allen u. J.T. Dewan: PR **80**, 181.

Al 51-1 S.G. Al-Salam: PR **84**, 254.

Al 51-2 K.W. Allen u. J.T. Dewan: PR **82**, 527.

Al 57-1 J.M. Alexander u. Ch.D. Coryell: PR **108**, 1274.

An 52-1 R.E. Anderson u. R.B. Duffield: PR **85**, 728.

An 58-1 M.P. Anikina, P.M. Aron: V.K. Gorškov, R.N. Ivanov, L.M. Križanski, G.M. Kukavadze, A.N. Murin, I.A. Reformacki u. B.V. Eršler: PUAE **15**, 446 (P/2040).

Au 55-1 J.M. Auclair, H.H. Landon u. M. Jacob, C. R. Acad. Sci., Paris **241**, 1935.

Au 58-1 J.M. Auclair: J. phys. Radium **19**, 68.

Ba 47-1 G.C. Baldwin u. G.S. Klaiber: PR **71**, 3.

Ba 51-1 R.E. Batzel u. G.T. Seaborg: PR **82**, 607.

Ba 54-1 R.E. Batzel: UCRL-4303.

Ba 54-2 F.R. Barclay, W. Galbraith, K. M. Glover, G.R. Hall u. W.J. Whitehouse: Proc. Phys. Soc., Lond., A **67**, 646.

Ba 55-1 B.N. Balujev, B.I. Gavrilov, G.N. Zacepina u. L.E. Lazareva: ŽETF **29**, 280; JETP **2**, 106 (1956).

Ba 55-2 B.P. Bannik u. Ju.S. Ivanov: Dokl. Akad. Nauk SSSR. **103**, 997; AEC-tr-2380.

Ba 56-1 R.M. Bartholomew u. A.P. Baerg: Can. J. Chem. **34**, 201.

Ba 57-1 B.P. Bannik, N.M. Kulikova, L.E. Lazareva u. V.A. Jakovlev: ŽETF **33**, 53; JETP **6**, 39 (1958).

Ba 57-2 G.A. Bat u. L.P. Kudrin: AE **3**, 15; SJAE **3**, 735 (1957); Kernenergie **1**, 346 (1958); J. Nucl. Energy **8**, 74 (1958/59).

Ba 57-3 B.P. Bayhurst, C.I. Browne, G.P. Ford, J.S. Gilmore, G.W. Knobeloch, E.J. Lang, M.A. Melnick u. C. Orth: PR **107**, 325.

Ba 58-1 A.I. Baz, N.M. Kulikova, L.E. Lazareva, N.V. Nikitina u. V.A. Semenov: PUAE **15**, 184 (P/2037).

Ba 59-1 R.M. Bartholomew, J.S. Martin u. A.P. Baerg: Can. J. Chem. **37**, 660.

Be 48-1 S. de Benedetti, J.E. Francis jr., W.M. Preston u. T.W. Bonner: PR **74**, 1645.

Be 51-1 G. Bernardini, E.T. Booth u. S.J. Lindenbaum: PR **83**, 669.

Be 52-1 G. Bernardini, E.T. Booth u. S.J. Lindenbaum: PR **85**, 826.

Be 53-1 G. Bernardini, R. Reitz u. E. Segrè: PR **90**, 573.

Be 55-1 G.E. Belovickij, T.A. Romanova, L.V. Souchov u. I.M. Frank: ŽETF **29**, 537; JETP **2**, 493 (1956).

Be 56-1 H.A. Bethe: Progress Nucl. Energy I **1**, 91.

Be 58-1 A.A. Berezin, G.A. Stoljarov, Ju. V. Nikoljskij u. I.E. Čelnokov, AE **5**, 659; SJAE **5**, 1604 (1958); Kernenergie **2**, 1022 (1959).

Bi 53-1 W.F. Biller, UCRL-2067

Bi 56-1 C.B. Bigham, CRP-642-A (AECL-329), S. 111.

Bi 58-1 D.R. Bidinosti, H.R. Fickel u. R.H. Tomlinson: PUAE **15**, 459 (P/201).

Bl 43-1 F. Bloch u. H. Staub: AECD-3158.

Bl 52-1 J.M. Blatt u. V.F. Weisskopf: Theoretical Nuclear Physics, S. 317. New York: John Wiley & Sons. Theoretische Kernphysik, S. 273. Leipzig: B.G. Teubner 1959.

Bl 52-2 J.M. Blatt u. V.F. Weisskopf: Theoretical Nuclear Physics, S. 365. New York: John Wiley & Sons. Theoretische Kernphysik, S. 314. Leipzig: B.G. Teubner 1959.

Bl 59-1 L. Blumberg, J. Bahcall, D. Garrett u. R.B. Leachman: Bull. Amer. Phys. Soc. II **4**, 31.

Bo 37-1 N. Bohr u. F. Kalckar: Kgl. Danske Videnskab. Selskab, Mat.-fys. Medd. **14**, 10.

Bo 39-1 N. Bohr u. J.A. Wheeler: PR **56**, 426.

Bo 40-1 N. Bohr: PR **58**, 864.

Bo 52-1 T.W. Bonner, R.A. Ferrell u. M.C. Rinehart: PR **87**, 1032

Bo 56-1 Aa. Bohr: PUAE **2**, 151 (P/911).

Bo 57-1 L.M. Bollinger: TID-7547, S. 85.

Bo 58-1 L.M. Bollinger, R.E. Coté u. G.E. Thomas: PUAE **15**, 127 (P/687).

Bo 58-2 H.R. Bowman u. S.G. Thompson: PUAE **15**, 212 (P/652).

Bo 58-3 I.I. Bondarenko, B.D. Kuzminov, L.S. Kucajeva, L.I. Prochorova u. G.N. Smirenkin: PUAE **15**, 353 (P/2187).

Br 49-1 D.C. Brunton: PR **76**, 1798.

Br 50-1 D.C. Brunton u. G.C. Hanna: Can. J. Research A **28**, 190.

Br 50-2 D.C. Brunton u. W.B. Thompson: Can. J. Research A **28**, 498.

Br 53-1 F. Brown u. L. Yaffe: Can. J. Chem. **31**, 242.

Br 54-1 J.E. Brolley jr. u. W.C. Dickinson: PR **94**, 640.

Br 55-1 J.E. Brolley jr., W.C. Dickinson u. R.L. Henkel: PR **99**, 159.

Br 56-1 D.A. Bromley: CRP-642-A (AECL-329), S. 65.

Br 56-2 F. Brown, M.R. Price u. H.H. Willis: J. Inorg. Nucl. Chem. **3**, 9.

Bu 56-1 G.R. Burbidge, F. Hoyle, E.M. Burbidge, R.F. Christy u. W.A. Fowler: PR **103**, 1145.

Bu 56-2 J.P. Butler, T.A. Eastwood, H.G. Jackson u. R.P. Schuman: PR **103**, 965.

Bu 56-3 J.P. Butler, M. Lounsbury u. J.S. Merritt: Can. J. Chem. **34**, 253.

Bu 58-1 L.R. Bunney, E.M. Scadden, J.O. Abriam u. N.E. Ballou: PUAE **15**, 449 (P/643).

Bu 58-2 L.R. Bunney, E.M. Scadden, J.O. Abriam u. N.E. Ballou: PUAE **15**, 444 (P/644).

Bu 58-3 J.P. Butler, B.J. Bowles u. F. Brown: PUAE **15**, 156 (P/6).

Ca 51-1 A.G.W. Cameron u. L. Katz: PR **84**, 608.

Ca 56-1 A.G.W. Cameron: CRP-642-A (AECL-329), S. 189.

Ca 57-1 A.G.W. Cameron: CRP-690 (AECL-433).

Ch 54-1 O. Chamberlain, G.W. Farwell u. E. Segrè: PR **94**, 156.

Ch 54-2 G.R. Choppin, S.G. Thompson, A. Ghiorso u. B.G. Harvey: PR **94**, 1080.

Ch 55-1 G.R. Choppin, B.G. Harvey, S.G. Thompson u. A. Ghiorso: PR **98**, 1519.

Ch 56-1 G.R. Choppin, B.G. Harvey, D.A. Hicks, J. Ise jr. u. R.V. Pyle: PR **102**, 766.

Cl 58-1 K.M. Clarke: ANL-5853.

Co 53-1 Ch. D. Coryell: Ann. Rev. Nucl. Sci. **2**, 305.

Co 54-1 B.L. Cohen, W.H. Jones, G.H. McCormick u. B.L. Ferrell: PR **94**, 625.

Co 55-1 B.L. Cohen, B.L. Ferrell-Bryan, D.J. Coombe u. M.K. Hullings: PR **98**, 685.

Co 56-1 B.L. Cohen, A.F. Cohen u. Ch. D. Coley: PR **104**, 1046.

Co 58-1 B.L. Cohen u. C.B. Fulmer: Nucl. Phys. **6**, 547.

Co 58-2 C.T. Coffin u. I. Halpern: PR **112**, 536.

Co 59-1 J.P. Conner, R.L. Henkel u. J.E. Simmons: Bull. Amer. Phys. Soc. II **4**, 234.

Cr 56-1 L. Cranberg, G. Frye, N. Nereson u. L. Rosen: PR **103**, 662.

Cr 56-2 W.W.T. Crane, G.H. Higgins u. H.R. Bowman: PR **101**, 1804.

Cr 58-1 E.A.C. Crouch u. I.G. Swainbank: PUAE **15**, 464 (P/7).

Cu 57-1 J.G. Cuninghame: J. Inorg. Nucl. Chem. **5**, 1.

Cu 57-2 J.G. Cuninghame: J. Inorg. Nucl. Chem. **4**, 1.

Cu 58-1 J.G. Cuninghame: J. Inorg. Nucl. Chem. **6**, 181.

Da 59-1 V.F. Darovskich u. N.A. Perfilov: ŽETF **36**, 652; JEPT **9**, 456 (1959).

De 46-1 P. Demers: PR **70**, 974.

De 55-1 R.W. Deutsch: PR **97**, 1110.

De 58-1 G.F. Denisenko, N.S. Ivanova, N.R. Novikova, N.A. Perfilov, E.I. Prokoffieva u. V.P. Šamov: PR **109**, 1779.

Di 56-1 B.C. Diven, H.C. Martin, R.F. Taschek u. J. Terrell: PR **101**, 1012.

Do 54-1 E.M. Douthett u. D.H. Templeton: PR **94**, 128.

Do 58-1 I. Dostrovsky, P. Rabinowitz u. R. Bivins: PR **111**, 1659.

Do 58-2 I. Dostrovsky, Z. Fraenkel u. P. Rabinowitz: PUAE **15**, 301 (P/1615).

Dr 57-1 V.A. Druin, S.M. Polikanov u. G.N. Flerov: ŽETF **32**, 1298; JETP **5**, 1059 (1957).

Du 53-1 R.B. Duffield u. J.R. Huizenga: PR **89**, 1042.

Du 53-2 S.P. Dutta: Indian J. Phys. **27**, 547.

Du 58-1 R.B. Duffield, R.A. Schmitt u. R.A. Sharp: PUAE **15**, 202 (P/678).

Ea 56-1 T.A. Eastwood: CRP-642-A (AECL-329), S. 43.

Eg 56-1 P.A. Egelstaff u. D.J. Hughes: Progress Nucl. Energy I **1**, 55.

Er 57-1 B.G. Erozolimski: AE, Suppl. 1, S. 74; SJAE, Suppl. 1, S. 51 (1957); PNF, S. 64 (1958).

Fa 47-1 G. Farwell, E. Segrè u. G. Wiegand: PR **71**, 327.

Fa 54-1 A.W. Fairhall, I. Halpern u. E.J. Winhold: PR **94**, 733.

Fa 56-1 F.J.M. Farley: J. Nucl. Energy **3**, 33.

Fa 56-2 A.W. Fairhall: PR **102**, 1335.

Fa 58-1 A.W. Fairhall, R.C. Jensen u. E.F. Neuzil: PUAE **15**, 452 (P/677).

Fa 58-2 H. Faissner u. F. Gönnenwein: Z. Physik **153**, 257.

Fe 42-1 N. Feather: BR-335 A.

Fe 47-1 E. Fermi u. E. Teller: PR **72**, 399.

Fe 51-1 B.T. Feld, H. Feshbach, M.L. Goldberger, H. Goldstein u. V.F. Weisskopf: NYO-636.

Fe 51-2 M.H. Feldman, L.E. Glendenin u. R.R. Edwards: NNES IV **9**, 598.

Fi 54-1 P.R. Fields, M.H. Studier, L.B. Magnusson u. J.R. Huizenga: Nature, Lond. **174**, 265.

Fi 54-2 P.R. Fields, M.H. Studier, J.F. Mech, H. Diamond, A.M. Friedman, L.B. Magnusson u. J.R. Huizenga: PR **94**, 209.

Fi 55-1 P.R. Fields, J.E. Gindler, A.L. Harkness, M.H. Studier, J.R. Huizenga u. A.M. Friedman: PR **100**, 172.

Fi 56-1 P.R. Fields, M.H. Studier, H. Diamond, J.F. Mech, M.G. Inghram, G.L. Pyle, C.M. Stevens, S. Fried, W.M. Manning, A. Ghiorso, S.G. Thompson, G.H. Higgins u. G.T. Seaborg: PR **102**, 180.

Fl 53-1 W.H. Fleming u. H.G. Thode: PR **92**, 378.

Fl 58-1 N.N. Flerov, A.A. Berezin u. I.E. Čelnokov: AE **5**, 657; SJAE **5**, 1600 (1958); Kernenergie **2**, 1020 (1959).

Fl 58-2 R.G. Fluharty, M.S. Moore u. J.E. Evans: PUAE **15**, 111 (P/645).

Fl 58-3 G.N. Flerov, D.S. Kločkov, V.S. Skobkin u. V.V. Terentev: Dokl. Akad. Nauk SSSR. **118**, 69; Soviet Physics (Doklady) **3**, 79 (1958).

Fo 47-1 J.L. Fowler u. L. Rosen: PR **72**, 926.

Fo 52-1 J.L. Fowler, W.H. Jones u. J.H. Paehler: PR **88**, 71.

Fo 53-1 G.P. Ford: AECD-3597.

Fo 53-2 G.P. Ford u. C.W. Stanley: AECD-3551.

Fo 55-1 R.L. Folger, P.C. Stevenson u. G.T. Seaborg: PR **98**, 107.

Fo 56-1 P. Fong: PR **102**, 434.

Fo 58-1 B.M. Foreman jr.: UCRL-8223.

Fo 59-1 W.D. Foland u. R.D. Present: PR **113**, 613.

Fr 46-1 J. Frenkel: J. Phys. USSR. **10**, 533.

Fr 47-1 S. Frankel u. N. Metropolis: PR **72**, 914.

Fr 51-1 S.S. Friedland: PR **84**, 75.

Fr 52-1 J.S. Fraser: PR **88**, 536.

Fr 54-1 J.S. Fraser u. J.C.D. Milton: PR **93**, 818.

Fr 55-1 J.E. Francis u. R.L. Gamble: ORNL-1879, S. 20.

Fr 56-1 S.M. Fried, G.L. Pyle, C.M. Stevens u. J.R. Huizenga: J. Inorg. Nucl. Chem. **2**, 415.

Fr 58-1 K. Fritze, C.C. McMullen u. H.G. Thode: PUAE **15**, 436 (P/187).

Fu 57-1 C.B. Fulmer u. B.L. Cohen: PR **108**, 370.

Ge 54-1 M. Gell-Mann, M.L. Goldberger u. W.E. Thirring: PR **95**, 1612 .

Gh 52-1 A. Ghiorso, G.H. Higgins, A.E. Larsh, G.T. Seaborg u. S.G. Thompson: PR **87**, 163.

Gh 54-1 A. Ghiorso, S.G. Thompson, G.H. Higgins, B.G. Harvey u. G.T. Seaborg: PR **95**, 293.

Gh 55-1 A. Ghiorso, B.G. Harvey, G.R. Choppin, S.G. Thompson u. G.T. Seaborg: PR **98**, 1518.

Gh 56-1 A. Ghiorso: PUAE **7**, 15 (P/718).

Gi 54-1 J. Gindler u. R.B. Duffield: PR **94**, 759.

Gi 56-1 W.M. Gibson: UCRL-3493.

Gi 56-2 J.E. Gindler, J.R. Huizenga u. R.A. Schmitt: PR **104**, 425.

Gl 51-1 L.E. Glendenin, Ch. D. Coryell u. R.R. Edwards: NNES IV **9**, 489.

Gl 51-2 L.E. Glendenin, E.P. Steinberg, M.G. Inghram u. D.C. Hess: PR **84**, 860.

Gl 55-1 R.A. Glass, S.G. Thompson u. G.T. Seaborg: J. Inorg. Nucl. Chem. **1**, 3.

Gl 55-2 L.E. Glendenin u. E.P. Steinberg: J. Inorg. Nucl. Chem. **1**, 45.

Gl 56-1 R.A. Glass, R.J. Carr, J.W. Cobble u. G.T. Seaborg: PR **104**, 434.

Go 48-1 M.L. Goldberger: PR **74**, 1269.

Go 49-1 R.H. Goeckermann u. I. Perlman: PR **76**, 628.

Go 49-2 F.K. Goward, E.W. Titterton u. J.J. Wilkins: Nature, Lond. **164**, 661.

Go 55-1 V.I. Goldanskij, V.S. Penkina u. E.Z. Tarumov: ŽETF **29**, 778; JETP **2**, 677 (1956).

Go 56-1 W.M. Good u. E.O. Wollan: PR **101**, 249.

Gr 49-1 L.L. Green u. D.L. Livesey: Phil. Trans. Roy. Soc. Lond. A **241**, 323.

Gr 54-1 A.E.S. Green: PR **95**, 1006.

Gr 56-1 E. Gross: UCRL-3330.

Gr 56-2 J.A. Grundl u. J.R. Neuer: Bull. Amer. Phys. Soc. II **1**, 95.

Gr 57-1 W.E. Grummitt u. G.M. Milton: J. Inorg. Nucl. Chem. **5**, 93.

Gr 57-2 W. E. Grummitt u. G. M. Milton: CRC-694 (AECL-453).

Gu 57-1 S.R. Gunn, H.G. Hicks, H.B. Levy u. P.C. Stevenson: PR **107**, 1642.

Gu 59-1 R. Gunnink u. J.W. Cobble: PR **115**, 1247.

Ha 41-1 R.O. Haxby, W.E. Shoupp, W.E. Stevens u. W.H. Wells: PR **59**, 57.

Ha 51-1 G.C. Hanna, B.G. Harvey, N. Moss u. P.R. Tunnicliffe: PR **81**, 466.

Ha 53-1 R. Hagedorn u. W. Macke: Vorträge über kosmische Strahlung, herausgeg. von W. Heisenberg, S. 201. Berlin: Springer.

Ha 54-1 G.N. Harding: AERE-N/R-1438.

Ha 55-1 J.A. Harvey, D.J. Hughes, R.S. Carter u. V.E. Pilcher: PR **99**, 10.

Ha 55-2 J.E. Hammel u. J.F. Kephart: PR **100**, 190.

Ha 56-1 G.N. Harding: Proc. Phys. Soc., Lond. A **69**, 330.

Ha 56-2 G.N. Harding u. F.J.M. Farley: Proc. Phys. Soc., Lond. A **69**, 853.

Ha 56-3 J.A. Harvey u. J.E. Sanders: Progress Nucl. Energy I **1**, 1.

Ha 57-1 I.W. Hay u. T.D. Newton: Can. J. Phys. **35**, 195.

Ha 58-1 I. Halpern u. C.T. Coffin: PUAE **15**, 398 (P/642).

Ha 58-2 I. Halpern u. V.M. Strutinski: PUAE **15**, 408 (P/1513).

Ha 58-3 W.W. Havens jr. u. E. Melkonian: PUAE **15**, 99 (P/655).

Ha 59-1 I. Halpern: Nucl. Phys. **11**, 522.

He 55-1 K.M. Henry u. M.P. Haydon: CF-55-4-22.

He 56-1 R.L. Henkel u. J.E. Brolley jr.: PR **103**, 1292.

He 56-2 K.M. Henry u. M.P. Haydon: ORNL-2081, S. 108.

He 58-1 A. Hemmendinger: PUAE **15**, 344 (P/663).

He 59-1 R.L. Henkel u. J.E. Simmons: Bull. Amer. Phys. Soc. II **4**, 233.

Hi 52-1 N.M. Hintz u. N.F. Ramsey: PR **88**, 19.

Hi 52-2 D.L. Hill: PR **87**, 1034.

Hi 52-3 D.L. Hill: PR **87**, 1049.

Hi 53-1 D.L. Hill u. J.A. Wheeler: PR **89**, 1102.

Hi 53-2 D.M. Hiller u. D.S. Martin jr.: PR **90**, 581.

Hi 55-1 H.G. Hicks u. R.S. Gilbert: PR **100**, 1286.

Hi 55-2 H.G. Hicks, P.C. Stevenson, R.S. Gilbert u. W.H. Hutchin: PR **100**, 1284.

Hi 56-1 D.A. Hicks, J. Ise jr. u. R.V. Pyle: PR **101**, 1016.

Hi 57-1 D.A. Hicks, J. Ise jr., R.V. Pyle, G. Choppin u. B. Harvey: PR **105**, 1507.

Hj 56-1 E. Hjalmar, H. Slätis u. S.G. Thompson: Ark. Fysik **10**, 357.

Ho 51-1 J.M. Hollander: UCRL-1396.

Ho 51-2 E.J. Hoagland u. N. Sugarman: NNES IV **9**, 1031.

Hu 51-1 H. Hurwitz jr. u. H.A. Bethe: PR **81**, 898.

Hu 53-1 J.R. Huizenga: ANL-5150.

Hu 53-2 E.K. Hulet, S.G. Thompson u. A. Ghiorso: PR **89**, 878.

Hu 53-3 E.K. Hulet: UCRL-2283.

Hu 54-1 J.R. Huizenga: PR **94**, 158.

Hu 54-2 J.R. Huizenga, J.E. Gindler u. R.B. Duffield: PR **95**, 1009.

Hu 56-1 J.R. Huizenga: PUAE **2**, 208 (P/836).

Hu 56-2 Ch. M. Huddleston: ANL-5609, S. 39.

Hu 57-1 J.R. Huizenga u. H. Diamond: PR **107**, 1087.

Hu 58-1 J.R. Huizenga: PR **109**, 484.

Hu 58-2 D.J. Hughes u. R.B. Schwartz: BNL-325. Second Edition.

Hy 57-1 E.K. Hyde u. G.T. Seaborg: Handbuch der Physik, Bd. **42**, S. **286**. Berlin: Springer.

In 58-1 D.R. Inglis: Ann. Physics **5**, 106.

Iv 55-1 N.S. Ivanova, N.A. Perfilov u. V.P. Šamov: Dokl. Akad. Nauk SSSR. **103**, 573; AERE-Lib/Trans-646.

Iv 56-1 N.S. Ivanova: ŽETF **31**, 413; JETP **4**, 365 (1957).

Iv 56-2 N.S. Ivanova u. I.I. Pjanov: ŽETF **31**, 416; JETP **4**, 367 (1957).

Iv 56-3 N.S. Ivanova: ŽETF **31**, 693; JETP **4**, 597 (1957).

Iv 57-1 N.S. Ivanova: AE, Suppl. 1, S. 115; SJAE, Suppl. 1, S. 76 (1957); PNF, S. 98 (1958).

Iv 57-2 R.N. Ivanov, V.K. Gorškov, M.P. Anikina, G.M. Kukavadze u. B.V. Eršler: AE **3**, 546; SJAE **3**, 1436 (1957); Kernenergie **1**, 887 (1958); J. Nucl. Energy **9**, 46 (1959).

Ka 48-1 S. Katcoff, J.A. Miskel u. Ch. W. Stanley: PR **74**, 631.

Ka 51-1 L. Katz u. A.G.W. Cameron: Can. J. Phys. **29**, 518.

Ka 53-1 S. Katcoff u. W. Rubinson: PR **91**, 1458.

Ka 55-1 L. Katz, T.M. Kavanagh, A.G.W. Cameron, E.C. Bailey u. J.W.T. Spinks: PR **99**, 98.

Ka 56-1 V.I. Kalašnikova, V.I. Lebedev, L.A. Mikajeljan u. M.I. Pevzner: AE **1**, Nr. 3, S. 11; SJAE **1**, 291 (1956); J. Nucl. Energy **4**, 67 (1957).

Ka 58-1 L. Katz, A.P. Baerg u. F. Brown: PUAE **15**, 188 (P/200).

Ka 58-2 S. Katcoff: Nucleonics **16**, Nr. 4, S. 78.

Ka 58-3 A.V. Kaljamin, A.N. Murin, B.K. Preobraženskij u. N.E. Titov: AE **4**, 196; SJAE **4**, 267 (1958); J. Nucl. Energy **9**, 165 (1959).

Ke 48-1 E.L. Kelly u. C. Wiegand: PR **73**, 1135.

Ke 54-1 R.N. Keller, E.P. Steinberg u. L.E. Glendenin: PR **94**, 969.

Ke 56-1 T.J. Kennett u. H.G. Thode: PR **103**, 323.

Ke 58-1 G.R. Keepin: AE **4**, 250; SJAE **4**, 339 (1958); Kernenergie **1**, 975 (1958); J. Nucl. Energy **7**, 13 (1958).

Kj 56-1 A. Kjelberg u. A.C. Pappas: Nucl. Phys. **1**, 322.

Kj 59-1 A. Kjelberg u. A.C. Pappas: J. Inorg. Nucl. Chem. **11**, 173.

Iv 58-1 N.S. Ivanova: ŽETF **34**, 1381; JETP **7**, 955 (1958).

Iv 58-2 N.S. Ivanova, V.I. Ostroumov u. R.A. Filov: PUAE **15**, 164 (P/2039).

Ja 49-1 A.H. Jaffey u. A. Hirsch: ANL-4286, S. 42.

Ja 56-1 J.D. Jackson: CRP-642-A (AECL-329), S. 125.

Je 58-1 R.C. Jensen u. A.W. Fairhall: PR **109**, 942.

Jo 53-1 W. John u. W.F. Fry: PR **91**, 1234.

Jo 55-1 L.G. Jodra u. N. Sugarman: PR **99**, 1470.

Jo 55-2 W.H. Jones, A. Timnick, J.H. Paehler u. T.H, Handley: PR **99**, 184.

Jo 56-1 W.H. Jones: ORO-162.

Jo 56-2 M. Jones, R.P. Schuman, J.P. Butler, G. Cowper, T.A. Eastwood u. H.G. Jackson: PR **102**, 203.

Jo 59-1 S.A.E. Johansson: Nucl. Phys. **12**, 449.

Ju 49-1 J. Jungerman u. S.C. Wright: PR **76**, 1112.

Ju 50-1 J. Jungerman: PR **79**, 632.

Ju 54-1 J. Jungerman u. H. Steiner: PR **93**, 949.

Ju 57-1 J.A. Jungerman u. H.M. Steiner: PR **106**, 585.

Ko 50-1 H.W. Koch, J. McElhinney u. E.L. Gasteiger: PR **77**, 329.

Ko 55-1 N.N. Kolesnikov u. S.I. Larkin: ŽETF **28**, 244; JETP **1**, 179 (1955).

Ko 56-1 V.A. Korotkova, P.A. Čerenkov u. I.V. Čuvilo: Dokl. Akad. Nauk SSSR. **106**, 811; Soviet Physics (Doklady) **1**, 104 (1956).

Ko 56-2 V.A. Korotkova, P.A. Čerenkov u. I.V. Čuvilo: Dokl. Akad. Nauk SSSR. **106**, 633; Soviet Physics (Doklady) **1**, 77 (1956).

Ko 57-1 V.P. Kovalev, V.N. Andrejev, M.N. Nikolajev u. A.G. Gusejnov: ŽETF **33**, 1069; JETP **6**, 825 (1958).

Ko 58-1 V.P. Kovalev: ŽETF **34**, 501; JETP **7**, 345 (1958).

Ko 58-2 V.P. Kovalev u. V.S. Stavinskij: ŽETF **35**, 787; JETP **8**, 545 (1959).

Ko 58-3 V.P. Kovalev u. V.S. Stavinskij: AE **5**, 649; SJAE **5**, 1588 (1958); Kernenergie **2**, 771 (1959).

Ko 58-4 B.S. Kovrigin u. K.A. Petržak: AE **4**, 547; Kernenergie **2**, 612 (1959).

Ko 59-1 B.S. Kovrigin, M. Ja. Kondratko u. K.A. Petržak: ŽETF **36**, 315; JETP **9**, 217 (1959).

Kr 52-1 A. Kramish: PR **88**, 1201.

Kr 55-1 P. Kruger u. N. Sugarman: PR **99**, 1459.

Kr 57-1 L.M. Križanskij, Ja. Malyj, A.N. Murin u. B.K. Preobraženskij: AE **2**, 276; SJAE **2**, 334 (1957); Kernenergie **1**, 58 (1958); J. Nucl. Energy **6**, 260 (1957/58).

Kr 58-1 L.M. Križanskij u. A.N. Murin: AE **4**, 77; SJAE **4**, 95 (1958); Kernenergie **1**, 1009 (1958).

Ku 55-1 B.V. Kurčatov, V.N. Mechedov, M. Ja. Kuznecova u. L.N. Kurčatova: Sessija Akad. Nauk SSSR. (Chemie), S. 120; Atomenergie (Chemie), S. 100 (1957); Conf. Acad. Sci. USSR. (Chemical Science), S. 79 (1956).

Ku 55-2 K. Kumar u. M.A. Preston: Can. J. Phys. **33**, 298.

Ku 55-3 B.V. Kurčatov, V.N. Mechedov, N.I. Borisova, M. Ja. Kuznecova, L.N. Kurčatova u. L.V. Čistjakov: Sessija Akad. Nauk SSSR. (Chemie), S. 178; Atomenergie (Chemie), S. 148 (1957); Conf. Acad. Sci. USSR (Chemical Science), S. 111 (1956).

La 54-1 H. de Laboulaye, C. Tzara u. J. Olkowsky: J. phys. Radium **15**, 470.

La 55-1 L.E. Lazareva, B.I. Gavrilov, B.N. Valujev, G.N. Zacepina u. V.S. Stavinskij: Sessija Akad. Nauk SSSR. (Phys. u. Math.), S. 306; Atomenergie (Phys. u. Math.), S. 251 (1957); Conf. Acad. Sci. USSR. (Phys. and Math. Sciences), S. 217 (1956).

La 57-1 A.K. Lavruchina, L.P. Moskaleva, L.D. Krasavina u. I.M. Grečiščeva: AE **3**, 285; SJAE **3**, 1087 (1957); J. Nucl. Energy **8**, 231 (1958/59).

La 57-2 A.K. Lavruchina u. L.D. Krasavina: AE **2**, 27; SJAE **2**, 27 (1957); J. Nucl. Energy **5**, 236 (1957).

La 58-1 A.K. Lavruchina, L.D. Krasavina u. A.A. Pozdnjakov: Dokl. Akad. Nauk SSSR. **119**, 56; Soviet Physics (Doklady) **3**, 283 (1958).

La 59-1 A.K. Lavruchina, L.D. Revina u. E.E. Rakovskij: Dokl. Akad. Nauk SSSR. **125**, 532; Soviet Physics (Doklady) **4**, 361 (1959).

La 59-2 R.W. Lamphere: ORNL-2718, S. 18.

Le 50-1 K.J. LeCouteur: Proc. Phys. Soc., Lond. A **63**, 259.

Le 52-1 R.B. Leachman: PR **87**, 444.

Le 54-1 R.B. Leachman u. H.W. Schmitt: PR **96**, 1366.

Le 55-1 R.B. Leachman u. W.D. Schafer: Can. J. Phys. **33**, 357.

Le 56-1 R.B. Leachman: PUAE **2**, 193 (P/592).

Le 56-2 R.B. Leachman: PR **101**, 1005.

Le 57-1 R.B. Leachman u. C.S. Kazek jr.: PR **105**, 1511.

Le 58-1 R.B. Leachman: PUAE **15**, 229 (P/2467).

Le 58-2 R.B. Leachman: PUAE **15**, 331 (P/665).

Le 58-3 V.I. Lebedev u. V.I. Kalašnikova: AE **5**, 176; SJAE **5**, 1019 (1958); Kernenergie **2**, 662 (1959).

Le 58-4 V.I. Lebedev u. V.I. Kalašnikova: ŽETF **35**, 535; JETP **8**, 370 (1959).

Le 58-5 B.R. Leonard jr., E.J. Seppi u. S.J. Friesenhahn: HW-56919, S. 62.

Le 58-6 R.M. Lessler: UCRL-8439.

Le 59-1 B.R. Leonard jr., HW-59126, S. 3; B.R. Leonard jr. u. E.J. Seppi: Bull. Amer. Phys. Soc. II **4**, 31 (1959).

Le 59-2 J. Leroy: C. R. Acad. Sci., Paris **248**, 954.

Li 52-1 D.J. Littler: Proc. Phys. Soc., Lond. A **65**, 203.

Li 54-1 M. Lindner u. R.N. Osborne: PR **94**, 1323.

Li 56-1 M. Lindner u. R.N. Osborne: PR **103**, 378.

Lo 55-1 O.V. Ložkin, N.A. Perfilov u. V.P. Šamov: ŽETF **29**, 292; JETP **2**, 116 (1956).

Lo 55-2 O.V. Ložkin u. V.P. Šamov: ŽETF **28**, 739; JETP **1**, 587 (1955).

Lu 56-1 E.V. Luoma: UCRL-3495.

Ma 49-1 L. Marshall: PR **75**, 1339.

Ma 54-1 L. Marquez: Nuovo Cim. (9) **12**, 288.

Ma 54-2 L.B. Magnusson, M.H. Studier, P.R. Fields, C.M. Stevens, J.F. Mech, A.M. Friedman, H. Diamond u. J.R. Huizenga: PR **96**, 1576.

Ma 57-1 L. Marquez: Proc. Phys. Soc., Lond. A **70**, 546.

Ma 57-2 L. Marquez: Nuovo Cim. (10) **5**, 1646.

Ma 58-1 F.C. Maienschein, R.W. Peelle, W. Zobel u. T.A. Love: PUAE **15**, 366 (P/670).

Mc 51-1 J. McElhinney u. W.E. Ogle: PR **81**, 342.

Mc 54-1 G.H. McCormick u. B.L. Cohen: PR **96**, 722.

Mc 54-2 H. McManus, W.T. Sharp u. H. Gellman: PR **93**, 924.

Me 56-1 J.F. Mech, H. Diamond, M.H. Studier, P.R. Fields, A. Hirsch, C.M. Stevens, R.F. Barnes, D.J. Henderson u. J.R. Huizenga: PR **103**, 340.

Me 57-1 V.N. Mechedov: AE, Suppl. 1, S. 181; SJAE, Suppl. 1, S. 120 (1957); PNF, S. 153 (1958).

Me 58-1 J.W. Meadows: PR **110**, 1109.

Me 58-2 N. Metropolis, R. Bivins, M. Storm, A. Turkevich, J.M. Miller u. G. Friedlander: PR **110**, 185.

Me 58-3 N. Metrpolis, R. Bivins, M. Storm, J.M. Miller, G. Friedlander u. A. Turkevich: PR **110**, 204.

Mi 52-1 J.F. Miller: UCRL-1902.

Mi 56-1 J.C.D. Milton: CRP-642-A (AECL-329), S. 207.

Mi 57-1 E.V. Minarik u. V.A. Novikov: ŽETF **32**, 241; JETP **5**, 253 (1957).

Mi 58-1 J.C.D. Milton u. J.S. Fraser: PR **111**, 877; PUAE **15**, 216 (P/199) (1958).

Mi 58-2 A.K. Michul u. M.G. Petrašcu: NP-7060.

Mo 58-1 T.A. Mostovaja: PUAE **15**, 433 (P/2031).

Na 57-1 R. Nasuhoglu, S. Raboy, G.R. Ringo, L.E. Glendenin u. E.P. Steinberg: PR **108**, 1522.

Ne 49-1 A.S. Newton: PR **75**, 17.

Ne 52-1 N. Nereson: PR **85**, 600.

Ne 52-2 N. Nereson: PR **88**, 823.

Ne 55-1 W.E. Nervik u. G.T. Seaborg: PR **97**, 1092.

Ne 58-1 M.F. Netter, H. Faraggi, A. Garin-Bonnet, M.J. Julien, C. Corge u. J. Turkiewicz: PUAE **15**, 418 (P/1188).

Ni 53-1 D.B. Nicodemus u. H.H. Staub: PR **89**, 1288.

No 58-1 R.A. Nobles u. R.B. Leachman: Nucl. Phys. **5**, 211.

Ob 58-1 A.I. Obuchov: ŽETF **35**, 1042; JETP **8**, 727 (1959).

Og 51-1 W.E. Ogle u. J. McElhinney: PR **81**, 344.

Os 55-1 V.I. Ostroumov: Dokl. Akad. Nauk SSSR. **103**, 409; AERE-Lib/Trans-692.

Os 55-2 V.I. Ostroumov: Dokl. Akad. Nauk SSSR. **103**, 413; AEC-tr-2289.

Os 56-1 V.I. Ostroumov u. N.A. Perfilov: ŽETF **31**, 716; JETP **4**, 603 (1957).

Os 57-1 V.I. Ostroumov u. R.A. Filov: ŽETF **33**, 1335; JETP **6**, 1026 (1958).

Pa 53-1 A.C. Pappas: AECU-2806.

Pa 56-1 A.C. Pappas: PUAE **7**, 19 (P/881).

Pa 56-2 F.I. Pavlockaja u. A.K. Lavruchina: AE **1**, Nr. 5, S. 115; SJAE **1**, 791 (1956); J. Nucl. Energy **5**, 149 (1957).

Pa 58-1 B.D. Pate, J.S. Foster u. L. Yaffe: PUAE **15**, 149 (P/197); Can. J. Chem. **36**, 1691 (1958).

Pa 58-2 F.I. Pavlockaja u. A.K. Lavruchina: ŽETF **34**, 1058; JETP **7**, 732 (1958).

Pa 58-3 B.D. Pate: Can. J. Chem. **36**, 1707.

Pe 55-1 N.A. Perfilov, N.S. Ivanova, O.V. Ložkin, V.I. Ostroumov u. V.P. Šamov: Sessija Akad. Nauk SSSR. (Chemie), S. 79; Atomenergie (Chemie), S. 66 (1957); Conf. Acad. Sci. USSR. (Chemical Science), S. 55 (1956).

Pe 55-2 J.A. Petruska, H.G. Thode u. R.H. Tomlinson: Can J. Phys. **33**, 693.

Pe 55-3 N.A. Perfilov, O.V. Ložkin u. V.P. Šamov: ŽETF **28**, 655; JETP **1**, 439 (1955).

Pe 55-4 N.A. Perfilov u. N.S. Ivanova: ŽETF **29**, 551; JETP **2**, 433 (1956).

Pe 57-1 N.A. Perfilov: AE, Suppl. 1, S. 98; SJAE, Suppl. 1, S. 66 (1957); PNF, S. 84 (1958).

Pe 57-2 N.A. Perfilov, V.P. Šamov u. O.V. Ložkin: Dokl. Akad. Nauk SSSR. **113**, 75; Soviet Physics (Doklady) **2**, 117 (1957).

Pe 58-1 N.A. Perfilov u. Z.I. Solovjeva: AE **5**, 175; SJAE **5**, 1017 (1958); Kernenergie **2**, 661 (1959).

Pe 58-2 N.A. Perfilov u. G.F. Denisenko: ŽETF **35**, 631; JETP **8**, 438 (1959).

Ph 58-1 L. Phillips, R. Gatti, A. Chesne, L. Muga u. S. Thompson: Phys. Rev. Letters **1**, 215.

Pi 56-1 V.E. Pilcher, J.A. Harvey u. D.J. Hughes: PR **103**, 1342.

Po 56-1 C.E. Porter u. R.G. Thomas: PR **104**, 483.

Po 57-1 N.T. Porile u. N. Sugarman: PR **107**, 1422.

Po 57-2 N.T. Porile u. N. Sugarman: PR **107**, 1410.

Po 57-3 N.T. Porile: PR **108**, 1526.

Po 59-1 S.M. Polikanov u. V.A. Druin: ŽETF **36**, 744; JETP **9**, 522 (1959).

Pr 47-1 R.D. Present: PR **72**, 7.

Pr 58-1 A.N. Protopopov, Ju. A. Selickij u. S.M. Solovjev: AE **4**, 190; SJAE **4**, 256 (1958); Kernenergie **1**, 1077 (1958); J. Nucl. Energy **9**, 157 (1959).

Pr 58-2 A.N. Protopopov u. V.P. Ejsmont: AE **4**, 194; SJAE **4**, 265 (1958); Kernenergie **1**, 1081 (1958); J. Nucl. Energy **9**, 164 (1959).

Pr 58-3 A.N. Protopopov u. V.P. Ejsmont: ŽETF **34**, 250; JETP **7**, 173 (1958).

Pr 58-4 A.N. Protopopov u. B.M. Širjajev: ŽETF **34**, 331; JETP **7**, 231 (1958).

Pr 58-5 A.N. Protopopov, G.M. Tolmačev, V.N. Ušackij, R.V. Venediktova, I.T. Krisjuk, L.P. Rodionova u. G.V. Jakovleva: AE **5**, 130; SJAE **5**, 963 (1958); Kernenergie **2**, 732 (1959).

Pr 58-6 A.N. Protopopov u. M.V. Blinov: AE **5**, 71; SJAE **5**, 885 (1958); Kernenergie **2**, 590 (1959).

Pr 59-1 A.N. Protopopov, Ju. A. Selickij u. S.M. Solovjev: AE **6**, 67; Kernenergie **2**, 1026 (1959).

Pr 59-2 A.N. Protopopov, I.A. Baranov u. V.P. Ejsmont: ŽETF **36**, 920; JETP **9**, 650 (1959).

Pr 59-3 A.N. Protopopov u. B.M. Širjajev: ŽETF **36**, 954; JETP **9**, 674 (1959).

Ra 58-1 R. Ramanna u. P.N. Rama Rao: PUAE **15**, 361 (P/1633).

Re 55-1 Z.L. Reineks, J.D. Finegan u. R.S. Shankland: AECU-3141.

Re 55-2 G.W. Reed: PR **98**, 1327.

Re 58-1 C.W. Reich u. M.S. Moore: PR **111**, 929.

Re 59-1 R.B. Regier, W.H. Burgus u. R.L. Tromp: PR **113**, 1589.

Ri 52-1 H.G. Richter u. Ch. D. Coryell: AECU-2082, S. 40.

Ri 54-1 H.G. Richter u. Ch. D. Coryell: PR **95**, 1550.

Ri 56-1 S.E. Ritsema: UCRL-3266.

Ro 50-1 L. Rosen u. A.M. Hudson: PR **78**, 533.

Ro 57-1 L.D. Roberts, J.W.T. Dabbs u. G.W. Parker: ORNL-2302, S. 31.

Ro 58-1 L.W. Roeland, L.M. Bollinger u. G.E. Thomas: PUAE **15**, 440 (P/551).

Ro 58-2 L.D. Roberts, J.W.T. Dabbs u. G.W. Parker: ORNL-2430, S. 51.

Ry 56-1 S.G. Ryžanov: ŽETF **30**, 599; JETP **3**, 632 (1956/57).

Sa 56-1 G. de Saussure u. E.G. Silver: ORNL-2081, S. 105.

Sa 56-2 J.E. Sanders u. C.J. Kenward: J. Nucl. Energy **3**, 70.

Sa 56-3 V.L. Sailor: PUAE **4**, 199 (P/586).

Sc 54-1 R.A. Schmitt u. N. Sugarman: PR **95**, 1260.

Sc 57-1 R.A. Schmitt u. R.B. Duffield: PR **105**, 1277.

Se 47-1 R. Serber: PR **72**, 1114.

Se 52-1 G.T. Seaborg: PR **85**, 157.

Se 52-2 G.T. Seaborg: PR **88**, 1429.

Se 54-1 E. Segrè u. C. Weigand: PR **94**, 157.

Se 58-1 E.J. Seppi: HW-54591, S. 13.

Sh 50-1 R.L. Shurey: UCRL-793.

Sh 58-1 F.J. Shore u. V.L. Sailor: PUAE **15**, 118 (P/648).

Sh 59-1 R.A. Sharp u. A.C. Pappas: J. Inorg. Nucl. Chem. **10**, 173.

Sk 56-1 K. Skarsvåg: PUAE **2**, 185 (P/884).

Sk 57-1 V.V. Skljarevskij, D.E. Fomenko u. E.P. Stepanov: ŽETF **32**, 256; JETP **5**, 220 (1957).

Sk 58-1 D.M. Skyrme u. G.N. Harding: Nuovo Cim. (10) **9**, 1082.

Sk 59-1 V.V. Skljarevskij, E.P. Stepanov u. B.A. Medvedev: ŽETF **36**, 326; JETP **9**, 225 (1959).

Sm 56-1 A.B. Smith, A.M. Friedman u. P.R. Fields: PR **102**, 813.

Sm 56-2 A.B. Smith, P.R. Fields u. A.M. Friedman: PR **104**, 699.

Sm 57-1 A.B. Smith, P.R. Fields u. A.M. Friedman: PR **106**, 779.

Sm 57-2 A.B. Smith, P.R. Fields u. J.H. Roberts: PR **108**, 411.

Sm 58-1 A. Smith, P. Fields, A. Friedman u. R. Sjoblom: PR **111**, 1633.

Sm 58-2 A. Smith, P. Fields, A. Friedman, S. Cox u. R. Sjoblom: PUAE **15**, 392 (P/690).

Sm 58-3 G.N. Smirenkin, I.I. Bondarenko, L.S. Kucajeva, Ch. D. Miščenko, L.I. Prochorova u. B.P. Šemetenko: AE **4**, 188; SJAE **4**, 253 (1958); Kernenergie **1**, 1003 (1958); J. Nucl. Energy **9**, 155 (1959).

Sm 59-1 A.B. Smith, P.R. Fields, R.K. Sjoblom u. J.H. Roberts: PR **114**, 1351.

Sm 59-2 A. Smith, P. Fields u. R. Sjoblom: Bull. Amer. Phys. Soc. II **4**, 31.

St 49-1 Ch.W. Stanley u. S. Katcoff: J. Chem. Phys. **17**, 653.

St 54-1 E.P. Steinberg u. L.E. Glendenin: PR **95**, 431.

St 54-2 M.H. Studier u. J.R. Huizenga: PR **96**, 545.

St 54-3 E.P. Steinberg, L.E. Glendenin, M.G. Inghram u. R.J. Hayden: PR **95**, 867.

St 56-1 H.M. Steiner u. J.A. Jungerman: PR **101**, 807.

St 56-2 E.P. Steinberg u. L.E. Glendenin: PUAE **7**, 3 (P/614).

St 56-3 V.M. Strutinskij: ŽETF **30**, 606; JETP **3**, 638 (1956/57).

St 57-1 W.E. Stein: PR **108**, 94.

St 57-2 V.M. Strutinskij: AE **2**, 508; SJAE **2**, 621 (1957); Kernenergie **1**, 257 (1958); J. Nucl. Energy **7**, 239 (1958).

St 58-1 R.H. Stokes, J.A. Northrup u. K. Boyer: PUAE **15**, 179 (P/659).

St 58-2 P.C. Stevenson, H.G. Hicks, W.E. Nervik u. D.R. Nethaway: PR **111**, 886.

St 58-3 W.E. Stein u. S.L. Whetstone jr.: PR **110**, 476.

St 59-1 V.S. Stavinskij: ŽETF **36**, 629; JETP **9**, 437 (1959).

Su 50-1 N. Sugarman: PR **79**, 532.

Su 53-1 N. Sugarman u. A. Haber: PR **92**, 730.

Su 56-1 N. Sugarman, M. Campos u. K. Wielgoz: PR **101**, 388.

Su 57-1 T.T. Sugihara, P.J. Drevinsky, E.J. Troianello u. J.M. Alexander: PR **108**, 1264.

Sw 51-1 J.A. Swartout u. W.H. Sullivan: NNES IV **9**, 856.

Sw 55-1 W.J. Swiatecki: PR **100**, 936.

Sw 55-2 W.J. Swiatecki: PR **100**, 937.

Sw 56-1 W.J. Swiatecki: PR **101**, 97.

Sw 56-2 W.J. Swiatecki: PR **101**, 651.

Ša 55-1 V.P. Šamov: Dokl. Akad. Nauk SSSR. **103**, 593; AEC-tr-2308.

Ša 55-2 V.P. Šamov u. O.V. Ložkin: ŽETF **29**, 286; JETP **2**, 111 (1956).

Ša 57-1 V.P. Šamov: AE, Suppl. 1, S. 129; SJAE, Suppl. 1, S. 85 (1957); PNF, S. 110 (1958).

Ša 57-2 V.P. Šamov: ŽETF **33**, 346; JETP **6**, 268 (1958).

Ša 58-1 V.P. Šamov: ŽETF **35**, 316; JETP **8**, 219 (1959); PUAE **15**, 171 (P/2222) (1958).

Ta 50-1 S. Tamor: PR **77**, 412.

Ta 58-1 N.I. Tarantin, Ju. B. Gerlit, L.I. Guseva, B.F. Mjasojedov, K.V. Filippova u. G.N. Flerov: ŽETF **34**, 316; JETP **7**, 220 (1958).

Te 52-1 H.A. Tewes u. R.A. James: PR **88**, 860.

Te 57-1 J. Terrell: PR **108**, 783.

Te 59-1 J. Terrell: PR **113**, 527.

Th 47-1 H.G. Thode u. R.L. Graham: Can. J. Research A **25**, 1.

Th 57-1 T.D. Thomas: UCRL-3791.

Th 58-1 T.D. Thomas, B.G. Harvey u. G.T. Seaborg: PUAE **15**, 295 (P/1429).

Ti 49-1 E.W. Titterton u. F.K. Goward: PR **76**, 142.

Ti 50-1 E.W. Titterton u. T.A. Brinckley: Phil. Mag. (7) **41**, 500.

Ti 51-1 E.W. Titterton: PR **83**, 673.

Ti 51-2 E.W. Titterton: PR **83**, 1076.

Ti 51-3 E.W. Titterton: Nature, Lond. **168**, 590.

To 56-1 R.H. Tomlinson: CRP-642-A (AECL-329), S. 262.

Ts 47-1 Tsien San-Tsiang, Ho Zah-Wei, R. Chastel u. L. Vigneron: PR **71**, 382.

Ts 48-1 Tsien San-Tsiang: J. phys. Radium **9**, 6.

Tu 40-1 L.A. Turner: Rev. Mod. Phys. **12**, 1.

Tu 51-1 A. Turkevich u. J.B. Niday: PR **84**, 52.

Tu 53-1 A. Turkevich, J.B. Niday u. A. Tompkins: PR **89**, 552.

Va 55-1 A.A. Varfolomejev, A.S. Romanceva u. V.M. Kutukova: Dokl. Akad. Nauk SSSR. **105**, 693; AEC-tr-2386.

Va 57-1 R. Vandenbosch: UCRL-3858.

Va 58-1 R. Vandenbosch u. G.T. Seaborg: PR **110**, 507.

Va 58-2 R. Vandenbosch u. J.R. Huizenga: PUAE **15**, 284 (P/688).

Va 58-3 R. Vandenbosch, T.D. Thomas, S.E. Vandenbosch, R.A. Glass u. G.T. Seaborg: PR **111**, 1358.

Va 58-4 I.A. Vasilev u. K.A. Petržak: ŽETF **35**, 1135; JETP **8**, 795 (1959).

Vi 55-1 A.P. Vinogradov, I.P. Alimarin, V.I. Baranov, A.K. Lavruchina, T.V. Baranova, F.I. Pavlockaja, A.A. Bragina u. Ju.V. Jakovlev: Sessija Akad. Nauk SSSR. (Chemie), S. 97; Atomenergie (Chemie), S. 81 (1957); Conf. Acad. Sci. USSR. (Chemical Science), S. 65 (1956).

Vl 57-1 V.V. Vladimirskij, A.A. Panov, I.A. Radkevič u. V.V. Soklolvskij, AE **3**, 444; SJAE **3**, 1315 (1957); J. Nucl. Energy **7**, 169 (1958).

Vo 57-1 V.K. Voitoveckij, B.A. Levin u. E.V. Marčenko: ŽETF **32**, 263; JETP **5**, 184 (1957).

Vo 58-1 E. Vogt: PR **112**, 203.

Wa 44-1 K. Way: CP-2497.

Wa 48-1 K. Way u. E.P. Wigner: PR **73**, 1318.

Wa 48-2 R.K. Wakerling: UCRL-132.

Wa 49-1 K. Way u. N. Dismuke: ORNL-280.

Wa 52-1 B.E. Watt: PR **87**, 1037.

Wa 54-1 J.S. Wahl: PR **95**, 126.

Wa 55-1 A.C. Wahl: PR **99**, 730.

Wa 55-2 A.H. Wapstra: Physica **21**, 385.

Wa 58-1 A.C. Wahl: J. Inorg. Nucl. Chem. **6**, 263.

Wa 58-2 J. Wahl: AECD-4261.

Wa 58-3 A.H. Wapstra: Handbuch der Physik, Bd. 38/1, S. 1. Berlin: Springer.

We 53-1 G.W. Wetherill: PR **92**, 907.

Wh 50-1 W.J. Whitehouse u. W. Galbraith: Phil. Mag. (7) **41**, 429.

Wh 52-1 W.J. Whitehouse u. W. Galbraith: Nature, Lond. **169**, 494.

Wh 52-2 W.J. Whitehouse: Progress Nucl. Phys. **2**, 120.

Wh 56-1 J.A. Wheeler: Physica **22**, 1103.

Wh 56-2 J.A. Wheeler: PUAE **2**, 155 (P/593).

Wh 57-1 J.A. Wheeler: TID-7547, S. 146.

Wh 59-1 S.L. Whetstone jr.: PR **114**, 581.

Wi 52-1 W.J. Winhold, P.T. Demos u. I. Halpern: PR **87**, 1139.

Wi 53-1 D.R. WILES, B.W. SMITH, R. HORSLEY u. H.G. THODE: Can. J. Phys. **31**, 419.

Wi 54-1 D.R. WILES u. CH. D. CORYELL: PR **96**, 696.

Wi 56-1 E.J. WINHOLD u. I. HALPERN: PR **103**, 990.

Wi 56-2 L. WILETS u. D.M. CHASE: PR **103**, 1296.

Wi 59-1 J. WING, W.J. RAMLER, A.L. HARKNESS u. J.R. HUIZENGA: PR **114**, 163.

Wo 56-1 R. WOLFGANG, E.W. BAKER, A.A. CARETTO, J.B. CUMMING, G. FRIEDLANDER u. J. HUDIS: PR **103**, 394.

Wo 57-1 R.L. WOLKE u. J.R. GUTMANN: PR **107**, 850.

Ya 50-1 Y. YAMAGUCHI: Progress Theor. Phys., Japan **5**, 143.

Za 57-1 JU. S. ZAMJATNIN: AE, Suppl. 1, S. 27; SJAE, Suppl. 1, S. 21 (1957); PNF, S. 21 (1958).

Table 5.2 Measurement of the energy distribution and range of fission products. (Numbers in parentheses: E/MeV; in photofission: E_e/MeV.)

Fission process	Measurement of T_l, T_h for fission-product pairs	Measurement of ν_b, ν_h for fission-product pairs	Measurement of T for single fission products	Measurement of the range distribution
Fm^{254} spontan.	Sm 58-2			
Cf^{252} spontan.	Sm 56-1 Hi 57-1 Bo 58-2	Mi 58-1 St 58-3		
Cm^{244} spontan.	Sm 58-2			
Cm^{242} spontan.	Sm 58-2		Sh 50-1 Ha 51-1	
Pu^{242} spontan.	Sm 57-1			
Pu^{241} + n	Sm 57-1 (th)			
Pu^{240} spontan.	Mo 58-1		Se 54-1	
Pu^{239} + n	Br 50-2 (th) Mo 58-1 (th)	St 57-1 (th)	Se 54-1 (th) Wa 54-1 (th; 14)	
U^{238} + C^{12}				Po 59-1 (75)
U^{238} + n			Ju 49-1 (45; 90) Wa 54-1 (2.5; 14)	Be 55-1 (150 - 380)
U^{238} + p				Pe 55-1 (460; 660) Ša 55-2 (660) Iv 56-2 (140 - 660) Iv 57-1 (140 - 660) De 58-1 (350)
U^{238} + π^+				De 58-1 (280) Iv 58-1 (280) Iv 58-2 (280)
U^{238} + π				Be 55-1 (slow) Pe 55-1 (slow) Pe 55-4 (slow) De 58-1 (slow)
U^{238} + γ			Ko 56-1 (17.7) Ko 59-1 (12.5)	
U^{238} spontan.	Ko 58-4		Wh 50-1	
U^{235} + n	Br 50-1 (th) Wa 54-1 (14) Ko 58-4 (th)	St 57-1 (th)	Fo 47-1 (slow;≃1) Ju 49-1 (90) Fr 51-1 (2.5; 14) Wh 50-1 (th) Wa 54-1 (th; 14) Ko 59-1 (slow)	
U^{233} + n	Br 50-1 (th) Fr 54-1 (th)	St 57-1 (th)		
Th^{232} + n			Fo 47-1 (≃ 1) Ju 49-1 (45; 90)	
Th^{232} + γ			Ko 56-1 (17.7)	
Th^{229} + n	Sm 58-1 (th)			
Ra^{226} + n			No 58-1 (4 - 21)	
Bi^{209} + n			Ju 49-1 (90)	
Bi^{209} + p				Pe 55-1 (460; 660) Ša 55-2 (660) Da 59-1 (660)
Bi^{209} + π^-				Pe 55-1 (slow)
Au^{197} + C^{12}				Po 59-1 (75)
W + p				Pe 55-1 (460; 660) Ša 55-2 (660)
W + π^-				Pe 55-1 (slow)
Ag, Br + p				De 58-1 (180 - 660) Ša 58-1 (300 - 660)

Table 6.1. Measurements of the anisotropy of fission-fragment emissions. (Numbers in parenthesis: E/MeV, in column γ, if no other listing: E_e/MeV. If the lower limit was missing, measurement was started at about E^h.)

Target nucleus	Z-N*	Bombarding particle					
		γ	n	p	d	α	C^{12}
Am^{241}	oe	Ka 58-1 (8)	Pr 59-2 (14.7)				
Pu^{239}	eo	Ka 58-1 (8 - 20)	Pr 58-3 (14.8) Bl 59-1 (2.6 - 14.1) He 59-1 (0.5 - 5)	Co 58-2 (11)	Co 58-2 (22)	Co 58-2 (43)	
Np^{237}	oe	Ka 58-1 (8)	Br 54-1 (14) Br 55-1 (14)	Co 58-2 (11)	Co 58-2 (12 - 22)	Co 58-2 (25 - 43)	
U^{238}	ee	Re 55-1 (8) Wi 56-1 (- 16) Ba 57-1 (9.4 - 26.5) Ba 58-1 (6.5 - 26.5) Ka 58-1 (6 - 20)	Br 54-1 (14) Va 55-1 (4 - 17) He 56-1 (- 20) Os 56-1 (680) Pr 58-2 (14)	Co 55-1 (22) Lo 55-1/+(460, 660) Pe 55-1/+(460, 660) Co 58-2 (11) Me 58-1 (45 - 155)	Co 58-2 (22)	Co 58-2 (43)	Po 59-1 (75)
U^{236}	ee	Co 59-1 ($E\gamma$ = 6.14 MeV)					
U^{235}	eo	Wi 56-1 (- 11) Ka 58-1 (8)	Br 54-1 (14) Br 55-1 (th - 20.4) He 59-1 (0.5 - 5) La 59-2 (0.4 - 3.7)	Co 55-1 (22) Co 58-2 (11)	Co 58-2 (22)	Co 58-2 (43)	
U^{234}	ee		La 59-2 (0.4 - 3.7)				
U^{233}	eo	Ka 58-1 ($\mp$ 20)	Br 54-1 (14) Ro 57-1 (th) Bl 59-1 (2.6 - 14.1) He 59-1 (0.5 - 5)	Co 55-1 (22)			
Th^{232}	ee	Wi 52-1 (- 16) Fa 54-1 (16) Wi 56-1 (- 16) Fa 58-2 (15.8) Ka 58-1 (6.5 - 20)	Br 54-1 (14) He 56-1 (- 20)	Co 54-1 (22) Co 55-1 (22) Co 58-2 (11) Me 58-1 (45 - 155)	Co 58-2 (12 - 22)	Co 58-2 (20 - 43)	
Th^{230}	ee	Ka 58-1 (8)		Co 55-1 (22)			
Ra^{226}	ee				Co 58-2 (22)	Co 58-2 (43)	
Bi^{209}	oe			Po 57-2 (450) Wo 57-1 (450)		Co 58-2 (43)	
Au^{197}	oe						Po 59-1 (75)
Ta^{181}	oe			Po 57-2 (450)			

*e = even, o = odd

Table 7.21-1. Specific independent and specific cumulative yields of fission products for spontaneous and thermal fission

Fission process	Fission product	Specific independent yield	Specific cumulative yield	References
Cm^{242} spontan.	Cs^{136}	0.11 ± 0.02		St 54-1
$Pu^{239} + n$	Rb^{86}	$1.6 \cdot 10^{-4}$		St 56-2+
	J^{128}	$(2.4 \pm 0.2) \cdot 10^{-4}$		Ke 56-1
	J^{130}	$(2.0 \pm 0.1) \cdot 10^{-3}$		Ke 56-1
	Cs^{136}	0.015		St 56-2+
		$3.1 \cdot 10^{-3}$		St 56-2+
$U^{235} + n$	As^{78}	0.009		Kj 59-1
	Br^{80}	$\sim 10^{-4}$		Ke 56-1
	Br^{82}	$1.4 \cdot 10^{-4}$		Fe 51-2
		$1.6 \cdot 10^{-4}$		St 56-2+
		$\sim 6 \cdot 10^{-4}$		Ke 56-1
	Kr^{89}		0.96	Wa 58-1
	Kr^{90}		0.86	Wa 58-1
	Kr^{91}		0.59	Wa 58-1
	Kr^{92}		0.31	Wa 58-1
	Rb^{86}	$1.3 \cdot 10^{-5}$		St 56-2+
	Y^{90}	$< 8 \cdot 10^{-5}$		Gr 57-1
	Y^{91}	$< 9 \cdot 10^{-3}$		Re 55-2
	Nb^{96}	$9 \cdot 10^{-5}$		St 56-2+
		$1.4 \cdot 10^{-4}$		Wa 58-1+
	Tc^{98}	$3 \cdot 10^{-8}$		Wa 58-1+
	Rh^{102}	$< 1.7 \cdot 10^{-7}$		Sw 51-1
	Te^{131}	0.04 - 0.12		Wa 58-1+
		0.14		Wa 58-1+
		0.15 ± 0.07		Pa 56-1
	Te^{132}	0.36 ± 0.17		Pa 56-1+
	J^{128}	$(9.8 \pm 1.0) \cdot 10^{-5}$		Ke 56-1
	J^{130}	$(2.8 \pm 0.2) \cdot 10^{-4}$		Ke 56-1
	J^{131}	< 0.01		Wa 55-1
	J^{132}	< 0.01		Wa 55-1
	J^{133}	< 0.05		Wa 55-1
	J^{134}	0.11 ± 0.02		Wa 55-1
		0.13		Wa 58-1+
		0.18 ± 0.02		Pa 56-1+
		0.21		St 56-2+
	Xe^{133}	< 0.001		Ka 53-1
	Xe^{135}	0.027		Br 53-1
		0.035		Ka 53-1
		0.049		Ho 51-2
		0.051 ± 0.007		Pa 56-1+
	Xe^{136}	0.53		St 49-1
	Xe^{139}		0.82	Wa 58-1
	Xe^{140}		0.59	Wa 58-1
	Xe^{141}		0.21	Wa 58-1
	Xe^{143}		$8.5 \cdot 10^{-3}$	Wa 58-1
	Xe^{144}		$1.1 \cdot 10^{-3}$	Wa 58-1
	Cs^{136}	$1.0 \cdot 10^{-3}$		St 56-2+
	La^{140}	$< 7 \cdot 10^{-4}$		Gr 57-1
	La^{141}	~ 0.02		Fo 53-2
	Pm^{148}	$< 6.8 \cdot 10^{-5}$		Pa 56-1+
		$< 1.1 \cdot 10^{-4}$		St 56-2+
$U^{233} + n$	Br^{80}	$< 10^{-3}$		Ke 56-1
	Br^{82}	$(2.5 \pm 0.8) \cdot 10^{-3}$		Ke 56-1
	Y^{90}	$< 8 \cdot 10^{-5}$		Gr 57-1
	Nb^{96}	$\simeq 5 \cdot 10^{3}$		Pa 56-1+
	J^{128}	$(1.1 \pm 0.1) \cdot 10^{-3}$		Ke 56-1
	J^{130}	$(3.8 \pm 0.3) \cdot 10^{-3}$		Ke 56-1
	Cs^{136}	0.02		St 56-2+
	La^{140}	$3.8 \cdot 10^{-3}$		Gr 57-1

Table 7.21-2. Measurements of independent yields of fission products at bombardment energies E>5 MeV.
(Numbers in parentheses: E/MeV, in column γ: E_e/MeV.)

Target nucleus	Bombarding particle				
	γ	n	p	d	α
Pu^{239}		Ke 56*1 (Fission neutrons) Fr 58*1 (Fission neutrons)		Gi 56*1 (20,6)	
Np^{237}					Gi 56-1 (31.5; 45.7)
U^{238}	Se 54-1 (48 - 300)		Fo 55-1 (340) Hi 55-1 (70 - 340) Vi 55-1 (480) Pa 56-2 (680) Aa 57-1 (170) La 57-2+ (480)	Hi 55-1 (19 - 190) Al 57-1 (13.6) Sh 59-1 (10 - 25)	Hi 55-1 (50 - 380)
U^{236}				Le 58-6 (23.4)	
U^{235}		Fo 53-1 (14) Wa 55-1 (14)		Le 58-6 (14.7; 23.4)	Va 57-1 (18 - 46)
U^{233}				Gi 56-1 (23.4)	Th 57-1 (20 - 46)
Th^{232}		Tu 51-1 (Fission neutrons)	Kr 55-1 (450) Vi 55-1 (480) Pa 56-2 (680) La 57-2+ (480) Pa 58-1 (8 - 90)	Al 57-1 (13.6)	Fo 58-1 (15 - 46)
Bi^{209}			Jo 55-1 (75 - 450) Kr 55-1 (450) Vi 55-1 (480) Pa 56-2 (680) La 57-2+ (480) Po 57-2 (450)	Go 49-1 (190)	
Au^{197}			Kr 55-1 (450)		
Re			Kr 55-1 (450)		
Ta^{181}			Kr 55-1 (450) Po 57-2 (450)		
Ho^{165}			Kr 55-1 (450)		

Table 8.211. Mean number of neutrons emitted per fission for spontaneous and thermal fission. (Optimum values for spontaneous fission from B_o 58-3+.)

Nucleus	$\bar{\nu}$	References
Fm^{254}	4.05 ± 0.19	Ch 56-1
Cf^{254}	3.90 ± 0.14	Bo 58-3+
Cf^{252}	3.84 ± 0.12	Cr 56-2, Di 56-1, Hi 56-1, Bo 58-2
Cf^{246}	2.92 ± 0.19	Bo 58-3+
Bk^{249}	3.72 ± 0.16	Bo 58-3+
Cm^{244}	2.82 ± 0.09	Cr 56-2, Di 56-1, Hi 56-1
Cm^{242}	2.59 ± 0.11	Cr 56-2, Hi 56-1
Pu^{242}	2.28 ± 0.13	Cr 56-2, Hi 56-1
Pu^{240}	2.23 ± 0.05	Cr 56-2, Di 56-1, Hi 56-1, Bo 58-3+
Pu^{238}	2.28 ± 0.10	Cr 56-2, Hi 56-1
Pu^{236}	2.17 ± 0.20	Cr 56-2, Hi 56-1
U^{238}	2.30 ± 0.20	Li 52-1
	Thermal fission	
Target nucleus	$\bar{\nu}$	References
Am^{241}	3.14 ± 0.05	Le 58-3
Pu^{241}	3.06 ± 0.04	Hu 58-2+
Pu^{239}	2.90 ± 0.04	Hu 58-2+
U^{235}	2.47 ± 0.03	Hu 58-2+
U^{233}	2.51 ± 0.03	Hu 58-2+
Th^{229}	2.13 ± 0.03	Le 58-4

Table 8.212. Mean numbers of neutrons emitted per fission for fission by neutrons. (See Le 58-1+, Table 2 and 3 for details.)

Target nucleus	E_n/MeV	$\bar{\nu}$	References
Pu^{239}	14.2	4.75 ± 0. 4	Le 59-2
U^{233}	14.8	4.4 ± 0.45	Pr 58-6
Th^{232}	4.0	2.70 ± 0.10	Bo 58-3

Table 8.22. Measurements and computations of the energy spectra of prompt neutrons. (Numbers in parentheses: E_n/MeV. Otherwise, $E_n \simeq 0.025$ eV.)

Fission process	Spectrum measurement	T_n/MeV (optimum value from Te 59-1)	Q/MeV (optimum value from Ta 59-1)	Numerical computation of the spectrum according to the evaporation theory
Cf^{252} spontan.	Hj 56-1 Sm 57-2 Bo 58-2	2.2 ± 0.1	0.71	Le 57-1 Ko 58-2 Te 59-1
Pu^{241} + n	Sm 58-2			
Pu^{239} + n	Ne 52-2 Gr 56-2 Er 57-1+ Ko 57-1 Bo 58-3(4) Ko 58-1 (0.05 - 0.7)	2.00 ± 0.05	0.61	
U^{238} + n				Ba 57-2 (0 - 10)
U^{235} + n	Bl 43-1 Hi 52-2 Ne 52-1 Bo 52-1/+ Wa 52-1 Ni 53-1 Cr 56-1 Le 56-1+ Er 57-1+ Bo 58-3(4) Ko 58-1 (0.05 - 0.7)	1,935 ± 0.05	0.58	Le 56-2(0;3) Ko 58-2 Ko 58-3 Te 59-1
U^{233} + n	He 55-1 Gr 56-2 He 56-2 Er 57-1+ Ko 57-1 Ko 58-1 (0.05 - 0.7) Sm 58-2 Sm 59-1	1.96 ± 0.05	0.59	

Table 8.23. Measured probable emission of exactly ν neutrons per fission. (Results of various authors were averaged. In fission by neutrons, the neutron energy was 80 kev)

Fission process	Probable emission of the listed number of neutrons per fission									References
	0	1	2	3	4	5	6	7	8	
Cf^{252} spontan.	0.003	0.012	0.119	0.247	0.341	0.176	0.074	0.017	0.004	Di 56-1 Hi 56-1
Cm^{244} spontan.	0.005	0.104	0.286	0.340	0.211	0.039	0.014	0.000	0.000	Di 56-1 Hi 56-1
Cm^{242} spontan.	0.011	0.126	0.323	0.347	0.139	0.050	0.004	0.001		Hi 56-1
Pu^{242} spontan.	0.063	0.192	0.351	0.324	0.033	0.036				Hi 56-1
Pu^{240} spontan.	0.051	0.210	0.349	0.250	0.118	0.023	0.001	0.000	0.000	Ha 55-2 Di 56-1 Hi 56-1
Pu^{238} spontan.	0.044	0.175	0.348	0.237	0.124	0.036				Hi 56-1
Pu^{236} spontan.	0.062	0.156	0.38	0.28	0.096	0.033				Hi 56-1
Pu^{239} + n	-0.01	0.11	0.13	0.56	0.11	0.06	0.05	0.00	-0.01	Di 56-1
U^{235} + n	0.027	0.158	0.339	0.305	0.133	0.038	-0.001	0.001	0.000	Di 56-1
U^{233} + n	0.000	0.151	0.326	0.301	0.176	0.042	-0.010	0.006	-0.002	Di 56-1

Table 8.3 Measurements and computations for prompt gamma-radiation

Fission process	E_n	Measuring range T_γ/MeV	$\overline{N}_\gamma$	$\overline{\Sigma T_\gamma}$/MeV	Remarks	References
Cf^{252} spontan.		0.2 - 7	10.3	8.2	measured	Sm 56-2
			10	9	measured	Bo 58-2
				4.0	computed	Le 57-1
U^{238} + n	2.8 MeV			7.5 ± 1.1	measured	Pr 59-3
	14.7 MeV			7.5 ± 1.1	measured	Pr 59-3
U^{235} + n		0.1 - 10	7.51	7.46	measured	Fr 55-1
	0.025 eV	0.3 - 10	7.4 ± 0.8	7.2 ± 0.8	measured	Ma 58-1
	0.025 eV			3.8	computed	Le 56-2
	2.8 MeV			7.5 ± 1.1	measured	Pr 58-4
	3 MeV			4.1	computed	Le 56-2
	14.7 MeV			7.5 ± 1.1	measured	Pr 58-4

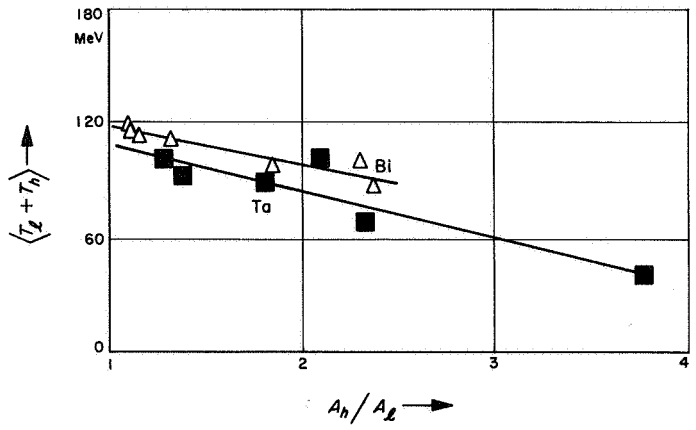

Fig. 5.21-1. Contour diagram for the thermal or spontaneous fission of the compound nucleus Pu^{242} (Sm 57-1)

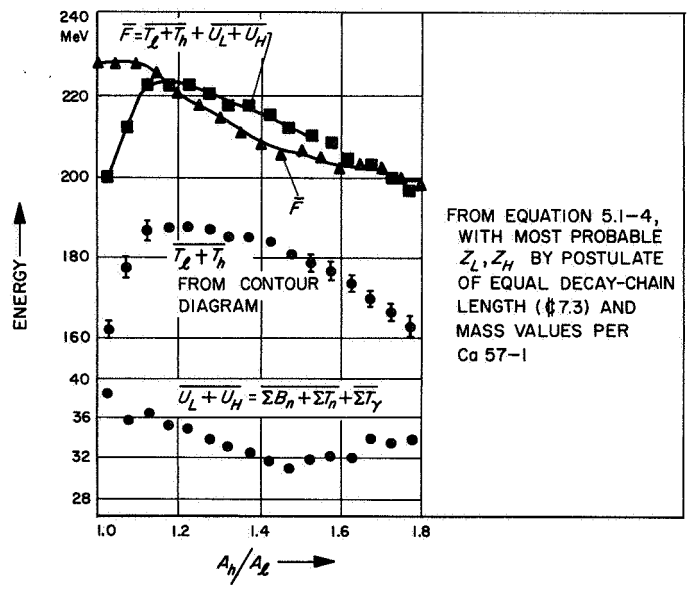

Fig. 5.22-2. Distribution of the total kinetic energy of the fission products for various areas of the fission ratio in the thermal or spontaneous fission of the compound nucleus Pu^{242} (Sm 57-1)

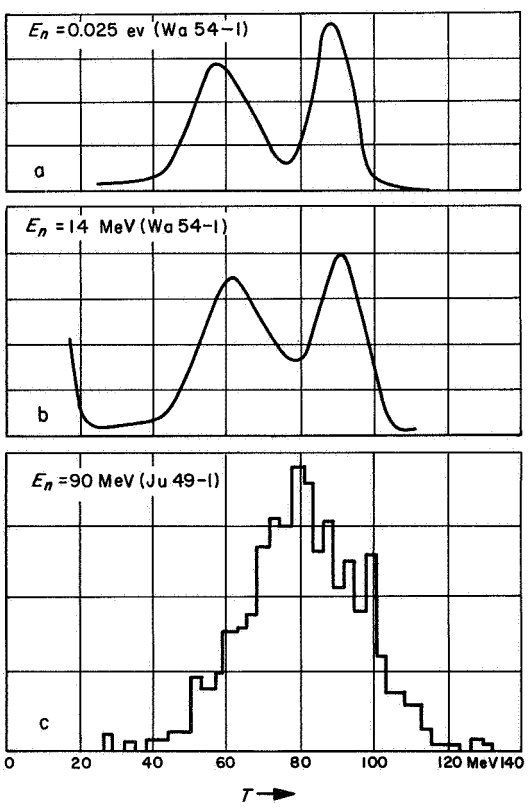

Fig. 5.3. Distribution of the kinetic energy of individual fission products in the fission of U^{235} by neutrons of various energies

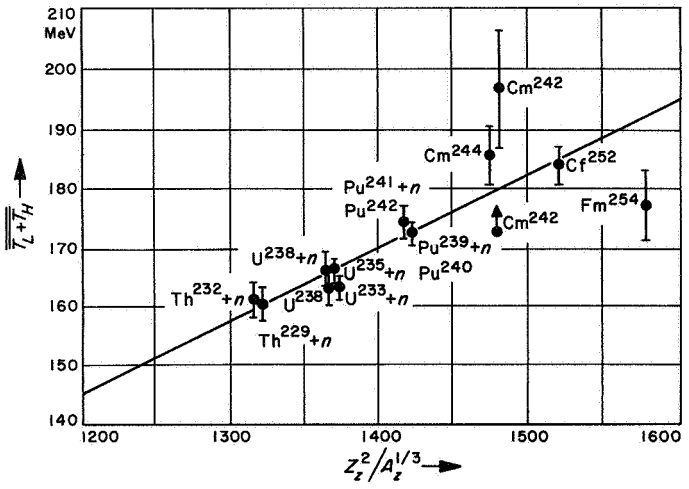

Fig. 5.53-1. Most probable total kinetic energy of the fission product as a function of the fission ratio for the fission of Bi and Ta by 450-MeV protons

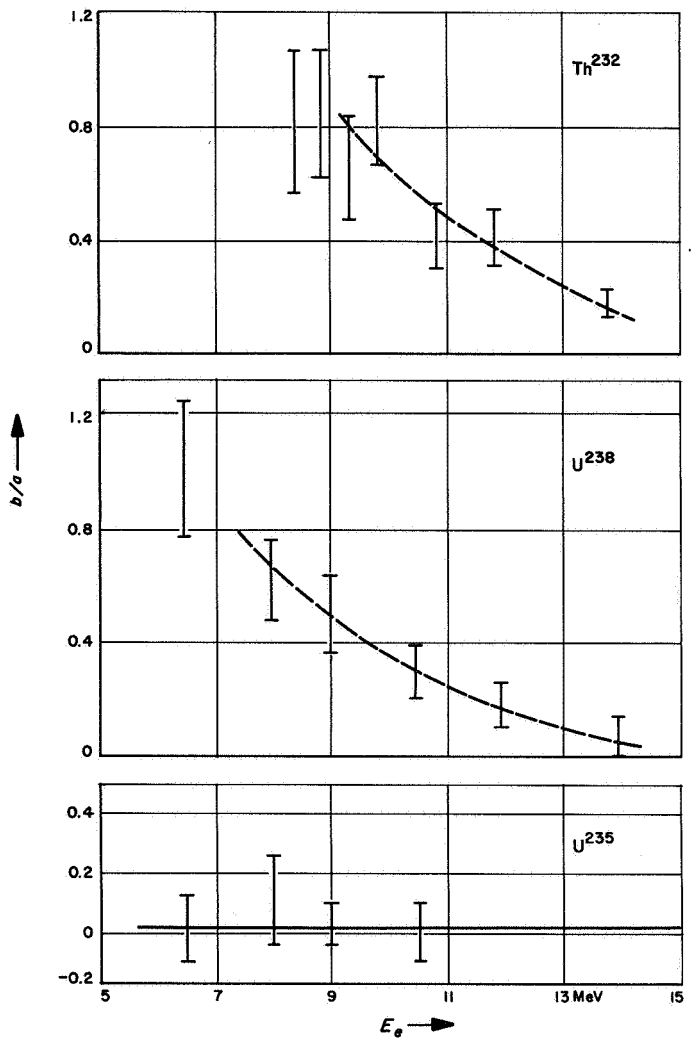

Fig. 5.53-2. Mean energy magnitudes (averaged like $\overline{T_l + T_h}$) as functions of the fission ratio for the spontaneous function of Cf^{252} (St 58-3)

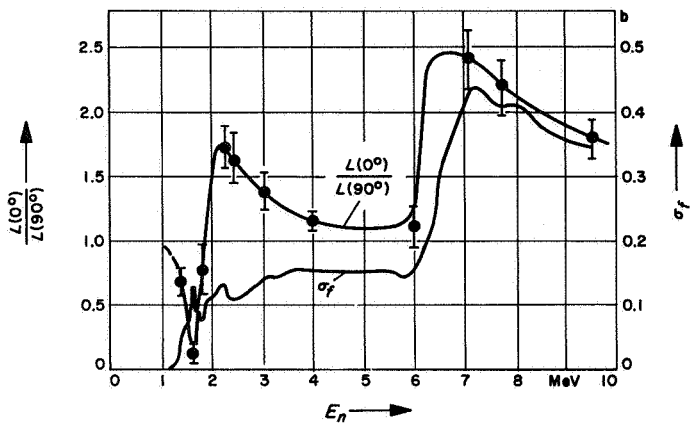

Fig. 5.6. Mean total kinetic energy of all fission-fragment pairs as a function of $Z_z^2/A_z^{1/3}$, computed from a number of data (Table 5.2; Te 59-1)

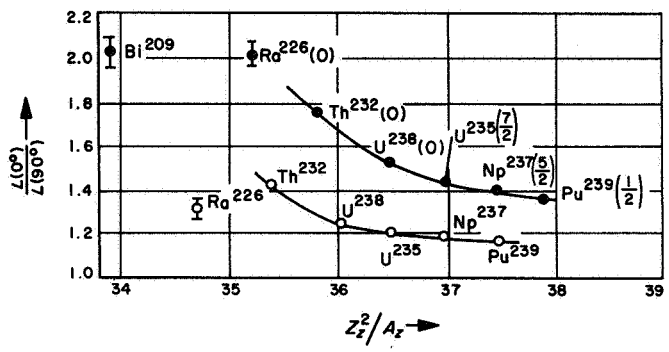

Fig. 6.21. Anisotropies in the photofission of various nuclei as a function of the maximum energy of the continuous radiation (Wi 56-1)

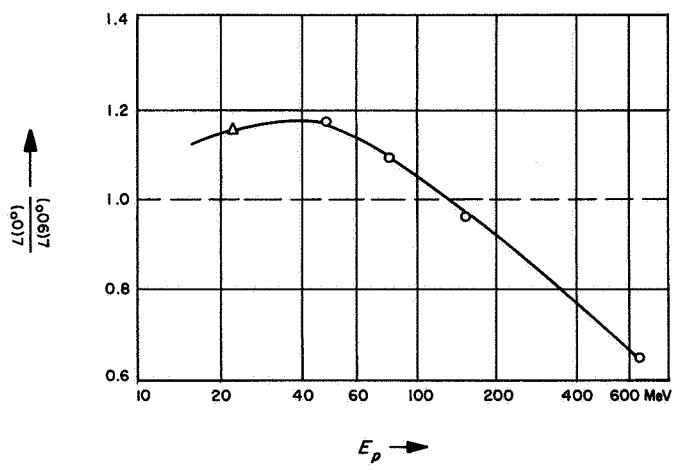

Fig. 6.4. Anisotropy of the fission-fragment emission and effective cross section for the fission of Th^{232} by neutrons as a function of their energy (He 56-1)

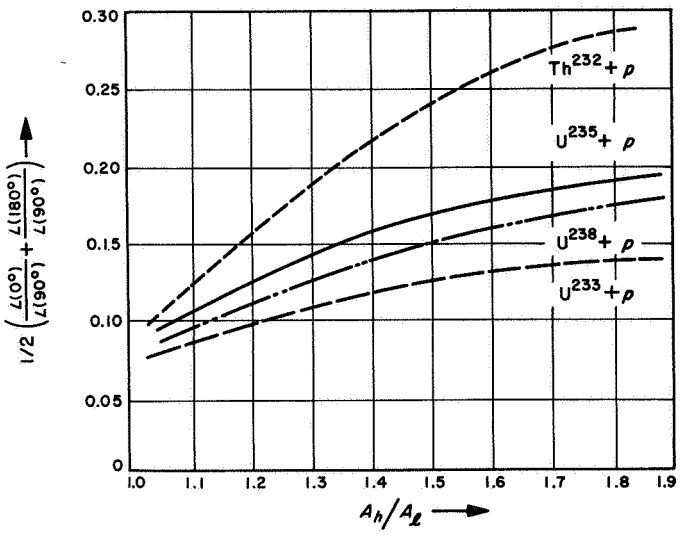

Fig. 6.52. Anisotropy of the fission-fragment emission for the fission of various target nuclei by deuterons and α-particles as a function of parameter Z^2/A of the compound nucleus (Co 58-2)

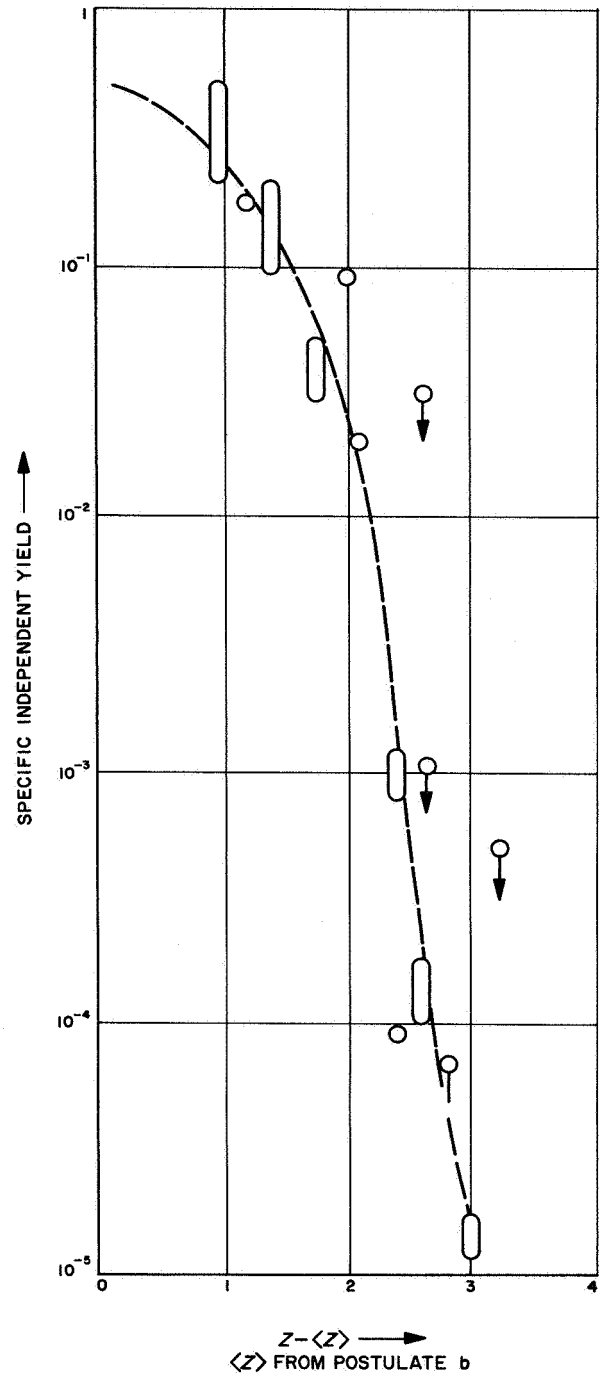

Fig. 6.53. Anisotropy of the fission-fragment emission in fission by very fast protons as a function of their energy (Ha 59-1)

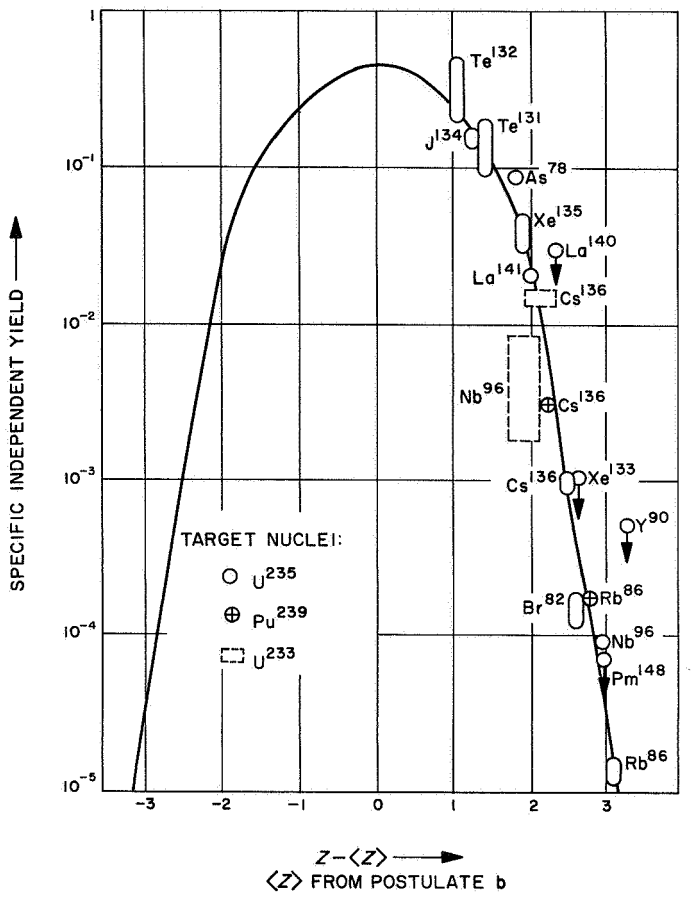

Fig. 6.54. Anisotropy in fission by 22-MeV protons as a function of the fission ratio (Co 55-1)

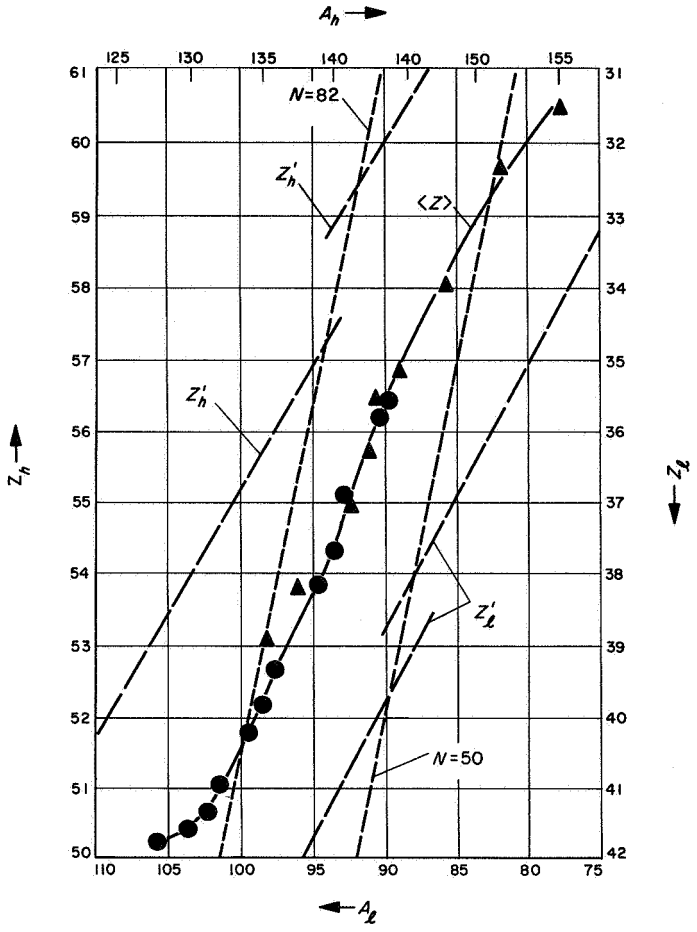

Fig. 7.41-1. Charge distribution for fixed mass number in the thermal fission of V^{235} according to postulate b

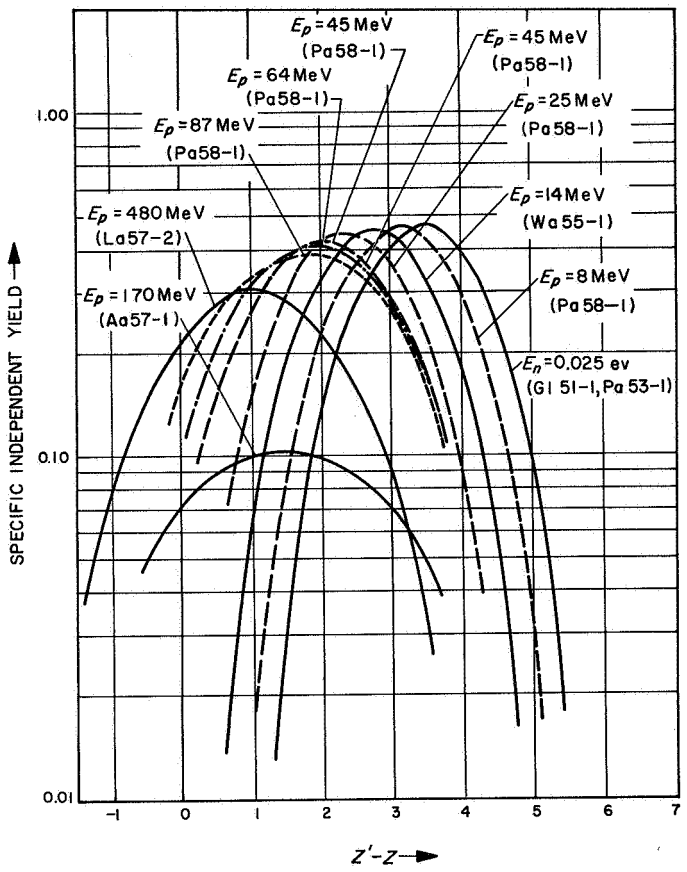

Fig. 7.41-2. Charge distribution for fixed mass number in thermal fission according to postulate b

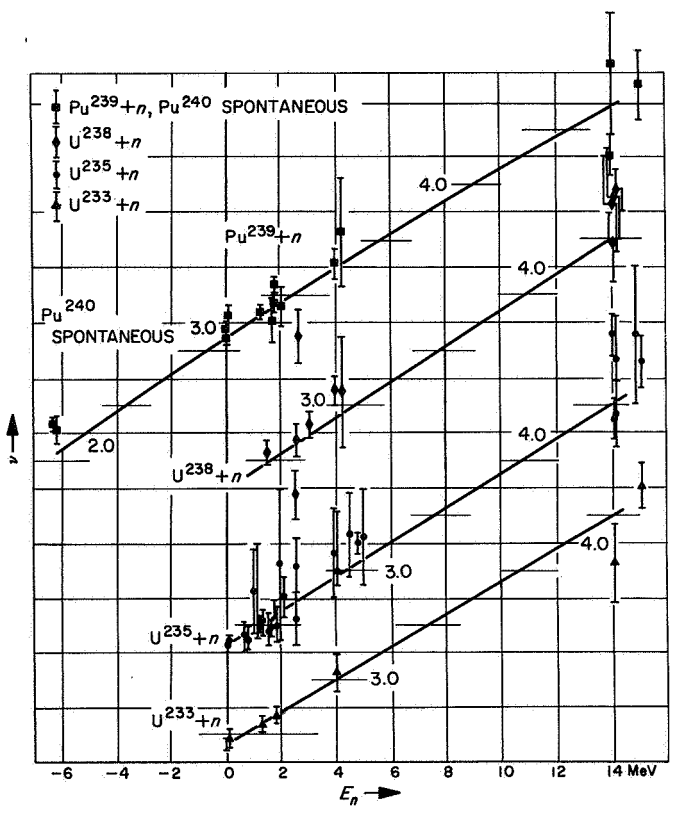

Fig. 7.41-3. The most probable charge < Z > for isobars of a mass number A as a function of A, according to Wa 58-1

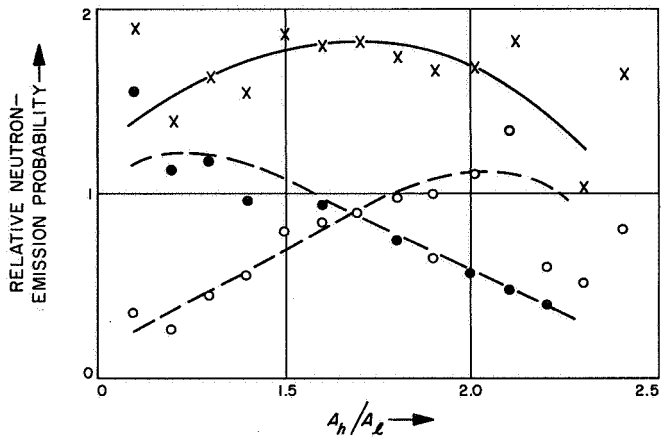

Fig. 7.42. Charge distribution for fixed mass number as a function of bombardment energy (Pa 58-1)

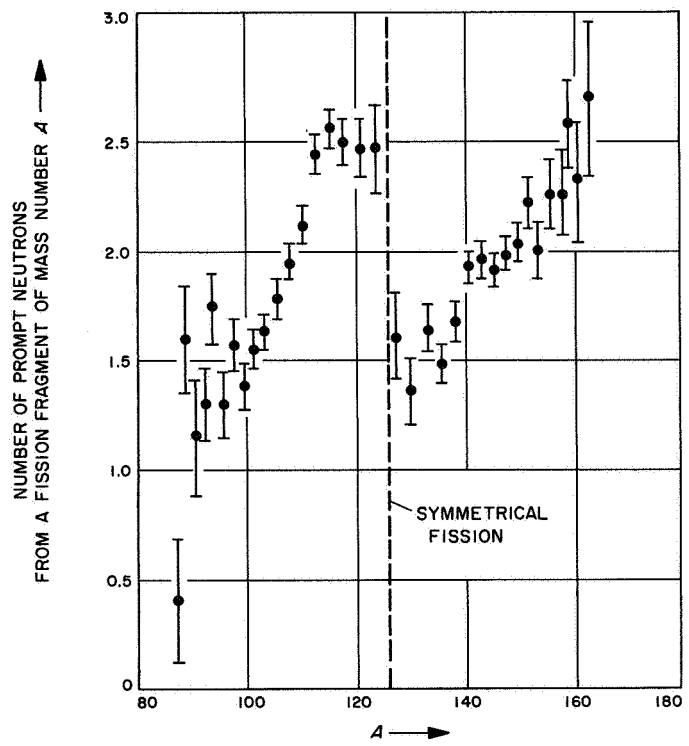

Fig. 8.212. $\overline{\nu}$ for several target nuclei and the spontaneously splitting nucleus Pu^{240} as a function of the bombarding-neutron energy (Le 58-1+)

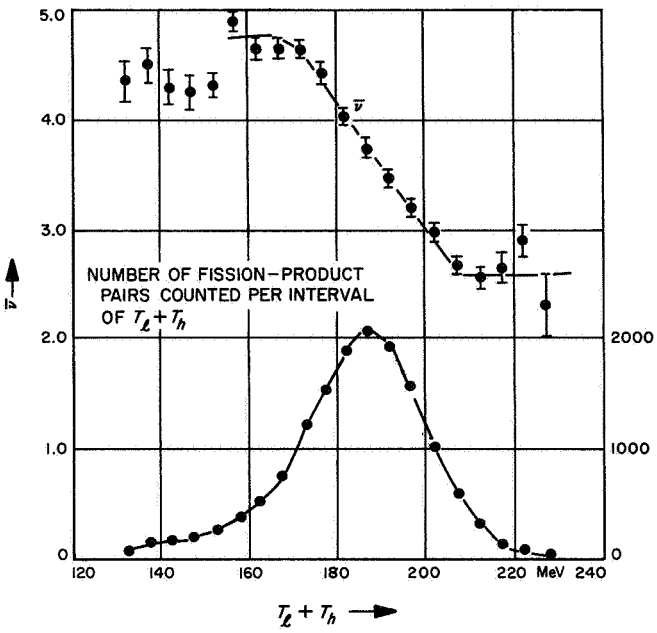

Fig. 8.213-1. Relative probability of neutron emission from light and heavy fission fragments and from both types of fission fragments as a function of the fission ratio for the thermal fission of U^{233} (Fr 54-1)

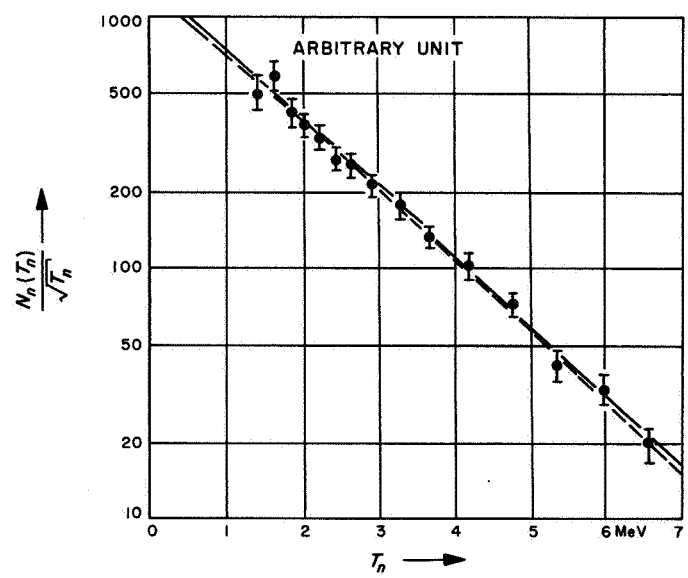

Fig. 8.213-2. Number of neutrons emitted from one fission fragment as a function of the mass number of this fission fragment in the spontaneous fission of Cf^{252} (Wh 59-1)

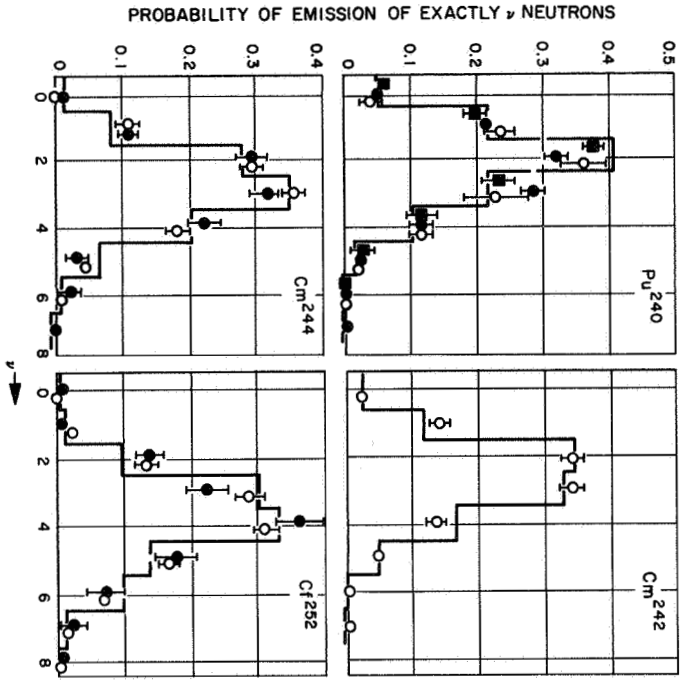

Fig. 8.214. $\overline{\nu}$ as a function of the total kinetic energy of the fission products in the spontaneous fission of Cf^{252}

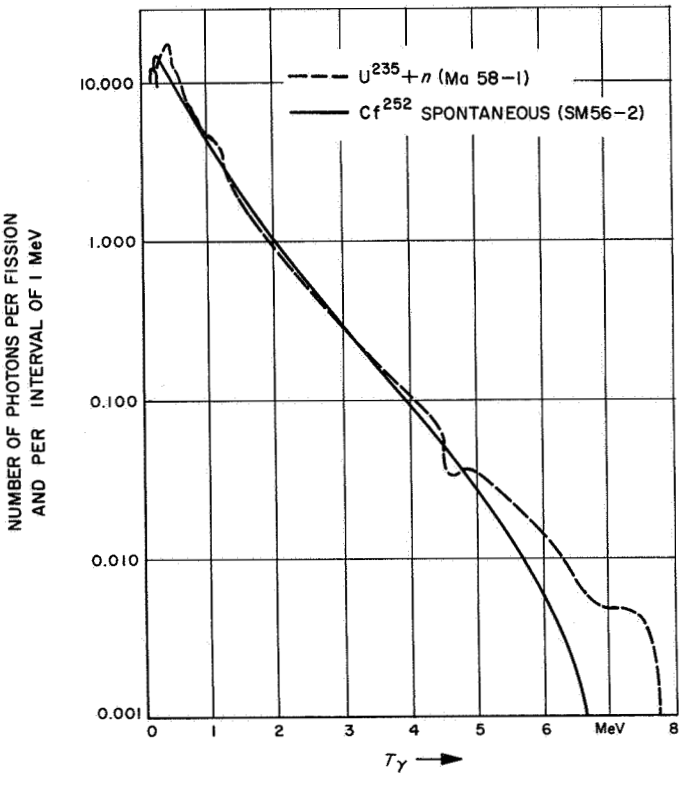

Fig. 8.22. Measured energy spectrum and computed energy spectra of prompt neutrons in the spontaneous fission of Cf^{252} (Te 59-1)

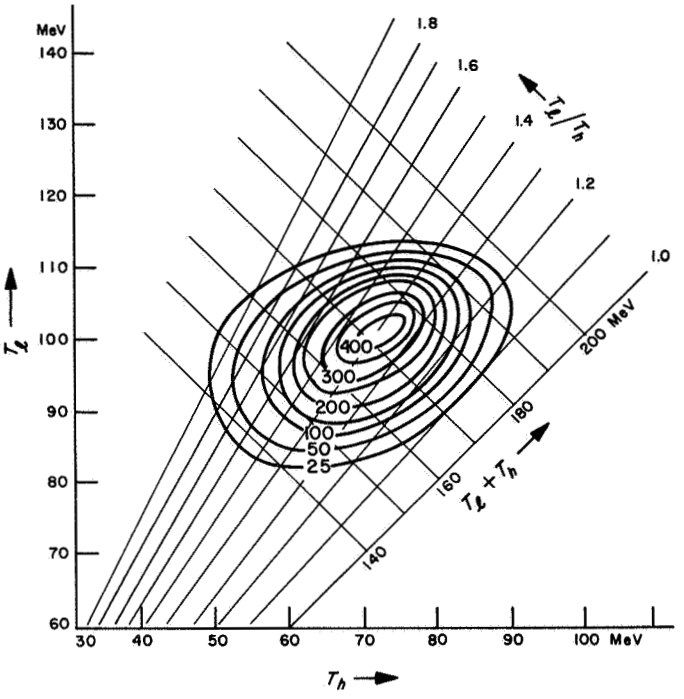

Fig. 8.23. Measured and computed probability for the emission of exactly ν neutrons as a function of ν for the spontaneous fission of several nuclei (Le 56-2)

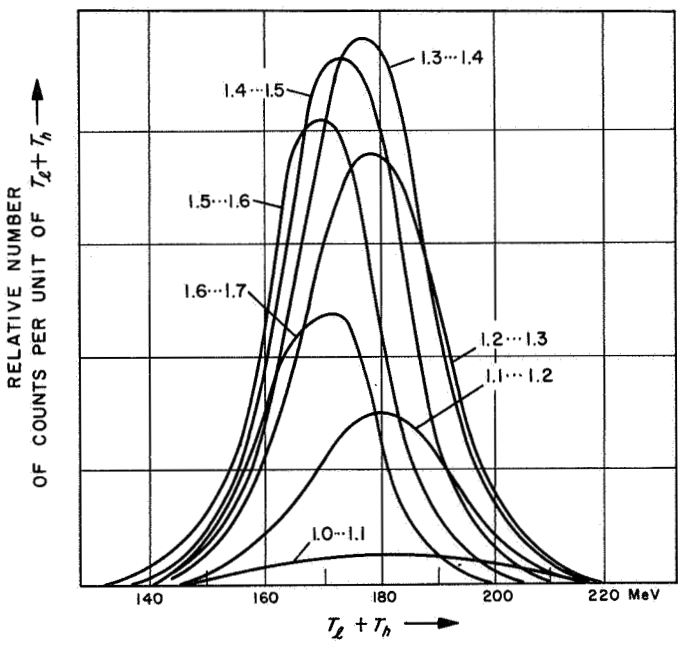

Fig. 8.32. Energy spectrum of the prompt gamma-radiation in the thermal fission of U^{235} and the spontaneous fission of Cf^{252}